ELSEVIER

Coordination Chemistry Reviews
183 (1999) 157–195

COORDINATION CHEMISTRY REVIEWS

Molecular and crystal engineering of a new class of inorganic cadmium-thiocyanate polymers with host–guest complexes as organic spacers, controllers, and templates

Hong Zhang [a,1], Ximin Wang [b], Kecong Zhang [b], Boon K. Teo [a,*]

[a] *Department of Chemistry, University of Illinois at Chicago, 845 W. Taylor St., 4500 SES, M/C111, Chicago, IL 60607, USA*

[b] *Department of Chemistry, Beijing Polytechnic University, Beijing 100022, People's Republic of China*

Received 14 May 1998; received in revised form 11 November 1998; accepted 30 November 1998

Contents

* Corresponding author. Tel.: +1-312-9969422; fax: +1-312-9969422.
[1] Also corresponding author.

PII: S0010-8545(98)00270-7

Abstract

This review provides an account of the structures of polymeric anionic cadmium-thiocyanate coordination solids with cationic crown-ether–metal complexes as spacers, controllers, and templates. Specifically, depending upon the size, shape, symmetry, and charge of the cationic host–guest complexes, this highly interesting series of coordination solids gives rise to a wide variety of structures, ranging from one-dimensional (1-D) single-chain structures (as exemplified by $[(18C6)K][Cd(SCN)_3]$ and $[(18C6)_2Na_2(H_2O)_2]_{1/2}[Cd(SCN)_3]$), to 1-D double-chain structures (as observed in $[(15C5)_2K][Cd_2(SCN)_5]$ and $[(15C5)_2Na_2(H_2O)_2]_{1/2}[Cd_2(SCN)_5]$), to two-dimensional (2-D) layered structures (as observed in $[(12C4)_2Cd][Cd_2(SCN)_6]$and $[(12C4)_2Cd][Cd_3(SCN)_8]$). These low-dimensional coordination solids exhibit highly anisotropic physical properties such as nonlinear optical (NLO) behavior. The arrangement and/or alignment of these polymeric cadmium-thiocyanates can be controlled and/or induced by the host–guest complexes. In this regard, for 1-D single- or double-chain cadmium-thiocyanate coordination solids, the cations serve as the spacer/controller, dictating the crystal structure and symmetry, thereby giving rise to desirable properties of these crystals such as nonlinear optical (NLO) behavior (as observed in $[(18C6)K][Cd(SCN)_3]$). In the case of 2-D cadmium-thiocyanate coordination solids, the cationic complex such as $[(12C4)_2Cd]^{2+}$ serves not only as the 'spacer' and 'controller' of the crystal packing, but also as an anisotropic 'template' for the formation of various layered

structures with highly interesting motifs. It is hoped that the inorganic polymers with organic spacers (IPOS) concept will not only lead to new and interesting materials but also to the development of new strategies in materials fabrication at the molecular engineering level and the discovery of new patterns of crystallization at the crystal engineering level. Furthermore, the general strategies and structural principles developed here can also be extended to other IPOS systems.

Keywords: Molecular and crystal engineering; Cadmium-thiocyanate polymers; Host–guest complexes; Spacer; Controller; Template

1. Introduction

One way to take advantage of the superior qualities of both inorganic, organic, and polymer materials is to combine them in the same compound. Recently, we developed a new class of hybrid materials based on inorganic polymers with organic spacers/controllers (IPOS) systems [1,2]. In particular, we have designed, synthesized, and structurally characterized a new series of hybrid crystalline materials of the general formula [H–G][M–L], where the cation [H–G] is a host (H)–guest (G) complex [3,4] and the anion [M–L] is a metal (M)–ligand (L) polymer, as depicted in Chart 1. These low-dimensional coordination solids exhibit anisotropic physical properties such as NLO behavior [5–7]. Our systematic structural studies on this series of coordination solids consisting of crown-ether–metal complexes and the anionic cadmium-thiocyanate polymers [8–14] led to a wide variety of structures, ranging from one-dimensional (1-D) single-chain structures (as exemplified by $[(18C6)K][Cd(SCN)_3]$ [1a] and $[(18C6)_2Na_2(H_2O)_2]_{1/2}[Cd(SCN)_3]$ [1a]), to 1-D double-chain structures (as observed in $[(15C5)_2K][Cd_2(SCN)_5]$ [1c] and $[(15C5)_2Na_2(H_2O)_2]_{1/2}[Cd_2(SCN)_5]$ [1c]), to two-dimensional (2-D) layered structures (as observed in $[(12C4)_2Cd][Cd_2(SCN)_6]$ [2a,b] and $[(12C4)_2Cd][Cd_3(SCN)_8]$ [2b]), depending upon the size, shape, symmetry, and charge of the cationic host–guest complexes. The arrangement and/or alignments of these polymeric cadmium-thiocyanates can be controlled and/or induced by the host–guest complexes. In this regard, for 1-D single- or double-chain cadmium-thiocyanate coordination solids,

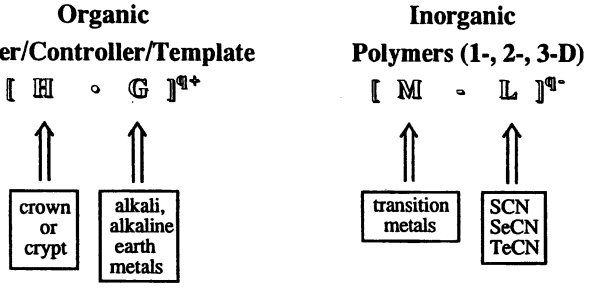

Chart 1. Four components of the IPOS system.

the cations serve as the spacer/controller, dictating the crystal structure and symmetry, thereby giving rise to desirable properties of these crystals such as NLO behavior (as observed in [(18C6)K][Cd(SCN)$_3$]). In the case of 2-D cadmium-thiocyanate coordination solids, the cationic complex such as [(12C4)$_2$Cd]$^{2+}$ dication serves not only as the 'spacer' and 'controller' of the crystal packing, but also as an anisotropic 'template' for the formation of various layered structures with unprecedented motifs [2].

This review provides an account of the structures of polymeric anionic cadmium-thiocyanate coordination solids with cationic crown-ether–metal complexes as spacers, controllers, and templates. It is hoped that the IPOS concept will lead to novel strategies in materials fabrication at the molecular engineering level as well as the discovery of new patterns of crystallization at the crystal engineering level. Furthermore, the general strategies and structural principles developed here can also be extended to other IPOS systems.

2. Inorganic polymers with organic spacers (IPOS) systems

The IPOS concept [1,2] combines the advantageous properties of inorganic, organic, and polymeric materials. It offers an excellent opportunity to synthesize isolated inorganic polymers of low dimensions (1- or 2-D) interspersed in an 'organic medium'. This particular IPOS series, as exemplified by the above-mentioned compounds, allows concomitant but separate molecular and crystal engineering [15–21] (i.e. design of molecular structure and crystal packing in two independent controls). In this section, we shall discuss briefly the chemical and structural characteristics of various components of the IPOS system.

2.1. Coordination modes of SCN^-, $SeCN^-$, and $TeCN^-$ ligands

The chalcogenocyanate ion, XCN^-, where X = S (thiocyanate), Se (selenocyanate), or Te (tellurocyanate), is a linear triatomic pseudohalide [8,9]. In the following discussions, as well as throughout this paper, we shall use SCN^- as a representative example of the chalcogenocyanate series.

SCN^- is a highly versatile ambidentate ligand with two donor atoms. It can coordinate through either the nitrogen or the sulfur atom, or both, giving rise to linkage isomers or polymers. The resonance structures are:

$$^-S{-}C{\equiv}N\ (\mathbf{A}) \leftrightarrow S{=}C{=}N^-\ (\mathbf{B}) \leftrightarrow {}^+S{\equiv}C{-}N^{2-}\ (\mathbf{C})$$

The relative importance of the resonance structures follows the trend $\mathbf{A} > \mathbf{B} \gg \mathbf{C}$. The modes of coordination of the SCN^- ligand can be classified as terminal or bridging, as depicted in Chart 2.

2.1.1. Terminal modes

There are two types of terminal coordination of SCN^- ligand: S-coordinated SCN^- (M–SCN) which is termed thiocyanate (type Ia, Chart 2) and N-coordi-

Type	Terminal	Type	Bridging
Ia	S-coordination S–C≡N | M (thiocyanate)	IIa	M–SCN–M
		IIb	M, M, SCN
		IIc	SCN, M, M
Ib	N-coordination S–C≡N–M (isothiocyanate)	IIIa	M, M, SCN–M
		IIIb	M–SCN, M, M
		IIIc	M, M–SCN, M
		IIId	SCN, M, M, M
		IVa	M, M, SCN, M, M
		IVb	M, M–SCN–M, M
		IVc	M–SCN, M, M, M
		Va	M, M–SCN, M, M, M
		Vb	M, M, SCN, M, M, M
		VI	M, M–SCN, M, M, M

Chart 2. Coordination modes of an ambidentate thiocyanate ligand.

nated SCN^- (M–NCS) which is called isothiocyanate (type Ib, Chart 2). Metal thiocyanates, M–S–C ≡ N, are usually bent with M–S–C angle of 100° (ranging from 80 to 110°) whereas in metal isothiocyanates, M–N ≡ C–S, the M–N–C angles are variable, though commonly with a M–N–C angle of around 150° (with a range of 110–180°). In either case, the S–C–N ligand is inevitably linear. While the M–N or M–S bond length depends on the nature and the electronic configura-

tion of the metal (M), the C–N and C–S distances are close to 1.16 and 1.62 Å, respectively [8,9].

Stereoisomers arising from N vs. S coordinated SCN^- (or any other ambidentate) ligands are termed linkage isomers. One interesting example is $Cu(SCN)_2$(tripyam) which has three forms: (a) the green $Cu(SCN)_2$(tripyam) [22] which has two S-bonded SCN^-; (b) the brown $Cu(NCS)_2$(tripyam) having two N-bonded NCS^-; and (c) the yellow–green Cu(NCS)(SCN) (tripyam) with one N- and one S-bonded thiocyanate ligand [22].

2.1.2. Bridging modes

On the basis of the three resonance structures of SCN^- discussed above, there are theoretically thirteen multidentate bridging modes, ranging from bi- to hexadentate (II–VI) for the ambidentate SCN^- ligand, as depicted in Chart 2 (here we ignore the highly unfavorable quadruple bridging of four atoms by either the S or the N atom.) However, not all of these bridging modes have been observed. The most commonly observed bridging modes are the bidentate (IIa–c) and the tridentate (IIIa,b) coordinations. Combinations of these coordination modes give rise to a variety of interesting metal thiocyanate structures as we shall discuss later.

2.2. Metal coordination

2.2.1. Hard versus soft acid–base coordination

The modes of metal coordination of chalcogenocyanates in general, and the thiocyanates in particular, are best understood in terms of the hard–soft acid–base concept developed by Pearson, Basolo, and Burmeister [23]. In accordance with the hard–soft acid–base concept, the S atom of the SCN^- ligand, being a soft base, preferentially coordinates to the soft acid whereas the N atom, being a hard base, preferentially coordinates to the hard acid. However, there are limitations to the hard–soft acid–base concept. Generally speaking, regardless of oxidation state or geometry, all of the metals in the first transition series, and all of the lanthanides and actinides exhibit only N-coordination. The first half of the second and third transition series also tend to be N-coordinated whereas at Rh(III) and Ir(III), there is a switch to S-coordination. This creates an interesting situation for the Zn–Cd–Hg triad. Here, the tetrahedral Zn(II) complexes tend to be N-bonded. The tetrahedral Hg(II) complexes are almost always S-bonded. Cd(II), in-between, becomes 'schizophrenic' [24], exhibiting both (S and N) bonding modes as well as a variety of coordination numbers as we shall see later.

2.2.2. Coordination numbers

The most common coordination numbers for metal thiocyanate complexes are 6 and 4, though less common coordination numbers such as 5, 3, 2 (low coordination) or 7, 8, 9 (high coordination), etc. are also formed. Generally, d^6 metal ions tend to form 6-coordinated octahedral complexes. Six-coordinated octahedral metal thiocyanate complexes can either be N-bonded, as exemplified by $Ni(NH_3)_4(NCS)_2$, or S-bonded, as in $[Rh(SCN)_6]^{3-}$. In these two examples, the hard acid Ni(II) is

coordinated by the hard base (N) terminus of the SCN^- ligand whereas the soft acid Rh(III) is coordinated by the soft base (S) terminus of the SCN^- ligand.

There are two types of 4-coordination: square planar and tetrahedral metal complexes. The former is generally adopted by d^8 metal complexes, as exemplified by $[Pt(SCN)_4]^{2-}$, whereas the latter by d^{10} metal complexes, such as $[Hg(SCN)_4]^{2-}$. Again, the N vs. S coordination is controlled by the hardness of the metal ions (in both of these examples, the soft Pt(II) and Hg(II) ions are S-coordinated).

Five-coordinated metal complexes can adopt either the trigonal bipyramidal structure, as exemplified by $[Zn(tren)NCS]^+(SCN)]^-$ [25] or the square pyramidal structure, as observed in $[Cd(NCS)_2Me_5(dien)]$ [26]. In both of these complexes, the metal ions are coordinated by N atoms only.

Three-coordinated metal thicyanate complexes adopt distorted trigonal planar structure, as observed in $Ph_3PHg(SCN)_2$ [27], though it has two long axial Hg···N contacts, making it a highly distorted trigonal bipyramidal structure.

Two-coordinated metal thiocyanate complexes are generally linear, as in CH_3HgSCN. The Hg in $Hg(SCN)_2$ may also be considered a linear molecule if the four exceedingly long Hg···N contacts at 2.81 Å are ignored (vide infra).

Other less common metal coordinations are: for example, the 7-coordinated pentagonal bipyramidal $(CH_3)_2Sn(NCS)_2$terpyridyl [28a], the 8-coordinated dodecahedral $K_4[Nd(NCS)_4(H_2O)_4](SCN)_3$ [28b], the 8-coordinated cubic $[Et_4N]_4[U(NCS)_8]$ [28c], the 9-coordinated $[Dy(NCS)_3(H_2O)_6]H_2O$ [28d], etc. High coordination numbers (≥ 7) are rare and are generally adopted by rare-earth elements.

2.2.3. Electronic effects

The electronic control of linkage isomerism comes from the competition for π bonding orbitals on the metal. For example, in $[(Ph_2PCH_2CH_2CH_2NMe_2)Pd(NCS)(SCN)]$ [29] (Chart 3), the phosphine is *trans* to N-bonded isothiocyanato group due to the fact that phosphine forms stronger π bonds with the π orbitals on the Pd^{2+} ion (than the N atom of the isothiocyanate ligand) whereas the N atom of amine is *trans* to S-bonded thiocyanato for the same reason.

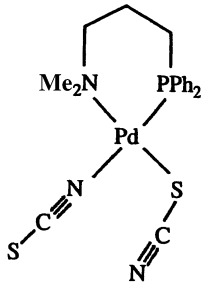

Chart 3.

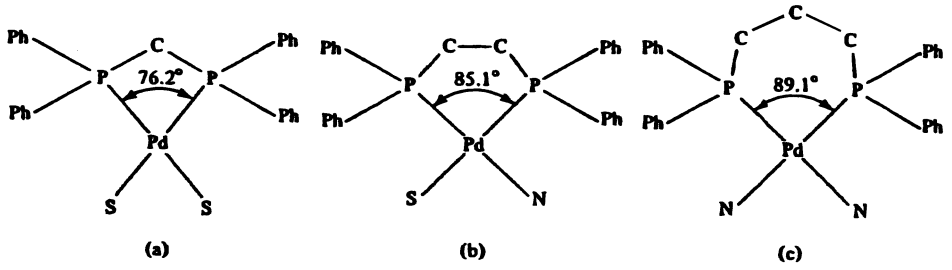

Chart 4. (Adapted from Ref. [30]).

2.2.4. Steric effects

Steric factors may also play an important role in the formation of thiocyanato vs. isothiocyanato linkage isomers as exemplified by the series of compounds of the general formula $LPd(SCN)_2$ where L is a bidentate phosphine ligand [30] depicted in Chart 4. Here, the six-membered chelate ring in $(Ph_2PCH_2CH_2CH_2PPh_2)Pd(NCS)_2$ allows an essentially unstrained angle of 89.1° at the palladium atom. The phosphines, being soft ligands, with significant π bonding with the Pd atom, are *trans* to N-bonded (hard ligand) isothiocyanato ligand, as expected. As the chelate ring is contracted to five atoms (in $(Ph_2PCH_2CH_2PPh_2)Pd(NCS)(SCN)$), and then to four atoms (in $(Ph_2PCH_2PPh_2)Pd(SCN)_2$), the electronic environment on the phosphine is essentially constant, but the steric hindrance are relaxed as the P–Pd–P bond angles decreased from 85.1 to 76.2°. Rearrangement of one and both of the thiocyanate groups occurs as the large sulfur atom is allowed more room around the Pd atom.

2.3. Metal–thiocyanate complexes, clusters, and polymers

A combination of variable metal coordination numbers (from 2 to 9), the ambidentate nature (N vs. S, type Ia,b, Chart 2), and the various bridging modes (13 bridging types, Chart 2) of the thiocyanate ligand gives rise to a wide variety of metal complexes, clusters, and polymers. Examples of simple metal thiocyanate complexes are cited above in the discussions of electronic and steric effects of metal coordination of the thiocyanate ligand.

We shall describe here two examples of cluster compounds containing thiocyanate bridges. Since chalcogenocyanate ligands are capable of forming a wide variety of bridges between metals (as depicted in Chart 2), they can form highly interesting cluster compounds. One example of dimeric clusters, $[(Pr_3P)PtCl(SCN)]_2$

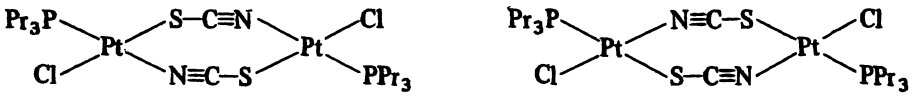

Chart 5.

[31], is portrayed in Chart 5. Yet another example is the tetrameric cubane-like $[(CH_3)_3Pt(SCN)]_4$ cluster [32]. Note that linkage isomers can also occur in bridged thiocyanate complexes as exemplified by the dimeric cluster (Chart 5).

The ambidentate nature and the highly versatile bridging modes of the SCN^- ligand also allow the formation of a wide variety of 1-, 2- and 3-D polymeric metal–thiocyanate structures. In the following sections, we shall focus our attention on the structures of IPOS systems of polymeric anionic cadmium-thiocyanate coordination solids, along with some discussions of related systems containing other metals or ligands.

2.4. Cationic host–guest complexes

The host–guest chemistry [3,4] refers to the binding of a wide variety of substrates in molecular cavities. In Fig. 1, we categorize the binding of the crown-ethers with alkali-metals into seven classes, according to the host:guest ratio as well as the match or mismatch of the metal ion with the size of the cavity of the crown-ether, along with representative examples.

The monomeric complexes (a), (b), and (c) all have a host:guest ratio of 1:1. Complex (a) has a disk-like structure which is formed when the size of the metal ion matches that of the crown-ether cavity as in $[(18C6)K][Cd(SCN)_3]$ (**1**) [1a]. In cases where the cavity size is slightly larger, a partial coiled complex (b) is formed as exemplified by $[(18C6)Na(H_2O)](SCN)$ [4a]. For even larger cavity size, the crown-ether may wrap around the metal ion to produce a 'coiled' structure (c) as observed in [(dibenzo-24C8)Na][$Cd(SCN)_3$] [1d]. Dimeric structures (d) and (e) have a host:guest ratio of 2:2. The dimeric structure (d) is formed when two crown-ether–metal ions are bridged two other ligands such as H_2O as observed in $[(15C5)_2Na_2(H_2O)_2]_{1/2}[Cd_2(SCN)_5]$ [1c] where Na^+ ion has the right size for 15C5. If, instead, the size of the crown-ether is larger than the metal ion, part of the crown-ether may function as the bridges in the dimer formation, as illustrated in dimeric structure (e) for $[(18C6)_2Na_2(H_2O)_2]_{1/2}[Cd(SCN)_3]$ (**2**) [1a]. If the size of the metal ion is significantly larger than the cavity size of the crown-ether, a sandwich structure (f) with a host:guest ratio of 2:1 may be formed as observed in $[(12C4)_2Na][Cd(SCN)_3]$ [1b]. On the other hand, if the cavity size of the crown-ether is substantially larger than the metal ions, a binuclear structure (g) may be formed as indeed observed in [(dibenzo-24C8)Na_2][*o*-$O_2NC_6H_4O]_2$ [4d]. Finally, it should be mentioned that other complex structures with other host:guest ratios are also possible (for comprehensive articles, see Ref. [3a–j]).

In order to enhance the formation of noncentrosymmetric space groups, a disk-like (a), partially coiled (b) or coiled (c) crown-ether–metal complexes should be used whereas the more spherical or more symmetrical crown-ether–metal cations such as dimeric (d) and (e), and sandwich (f) structures, should be avoided due to their tendency in forming centrosymmetric space groups. The utility of cationic crown-ether–metal complexes as spacers/controllers/templates in the crystal engineering of anionic cadmium-thiocyanate coordination solids will be discussed next.

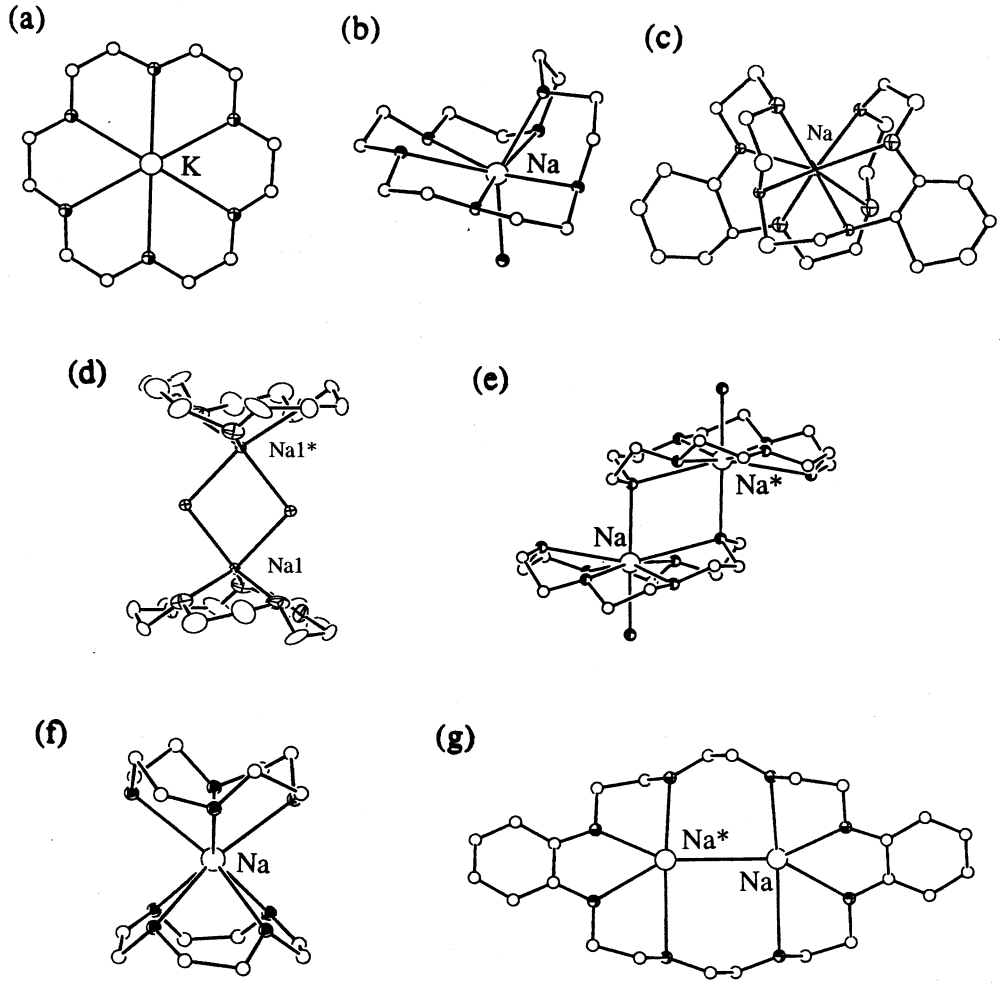

Fig. 1. Representative examples of seven categories of the crown-ether (host)–alkali-metal (guest) structures: (a) disk-like (host:guest = 1:1) as in [(18C6)K][Cd(SCN)$_3$] (**1**) [1a]; (b) partially coiled (1:1) as in [(18C6)Na(H_2O)](SCN) [4a]; (c) coiled (1:1) as in [(dibenzo-24C8)Na][Cd(SCN)$_3$] [1d]; (d) dimer (2:2) as in $[(15C5)_2Na_2(H_2O)_2]_{1/2}[Cd_2(SCN)_5]$ [1c]; (e) dimer (2:2) as in $[(18C6)_2Na_2(H_2O)_2]_{1/2}[Cd(SCN)_3]$ (**2**) [1a]; (f) sandwich (2:1) as in $[(12C4)_2Na][Cd(SCN)_3]$ (**3**) [1b]; and (g) two nuclei (1:2) as in [(dibenzo-24C8)Na_2][*o*-$O_2NC_6H_4O]_2$ [4d].

3. One-dimensional single-chain anionic cadmium-thiocyanate structures with cationic spacers/controllers

1-D anionic cadmium thiocyanate coordination solids are rather rare. Only a few examples of 1-D $[Cd(SCN)_3]^-$ and $[Cd(SCN)_4]^{2-}$ chain structures are known [1,10,11]. Fig. 2 depicts the structure of a representative anionic polymeric cadmium-thiocyanate chain observed in a number of 1-D cadmium-thiocyanate and

crown-ether–metal coordination solids [1b]. It can be seen that each Cd atom is octahedrally coordinated with three S and three N atoms (in *fac* configuration, i.e. N atoms are *trans* to the S atoms (and vice versa) due to the *trans* influence). The average Cd–S and Cd–N distances are 2.748 and 2.307 Å, and the average Cd–S–C and Cd–N–C angles are 97.1 and 150.9°, respectively. The SCN ligands are virtually linear (178.2(av)°) with S–C and C–N bond lengths of 1.640(av) and 1.147(av) Å, respectively. Cd atoms are linked by three SCN^- ligands, forming an infinite anionic zigzag polymeric chain, $[Cd(SCN)_3^-]_\infty$, which we shall refer to as a single-chain, with Cd···Cd distances of 5.41(av) Å and Cd···Cd···Cd angles of 162.2(av)°. The arrangements as well as the alignments of the anionic $[Cd(SCN)_3^-]_\infty$ zigzag single-chains are highly dependent upon the nature of cationic crown-ether–metal complexes, as we will discuss next.

3.1. Structures of [(18C6)K][Cd(SCN)$_3$] and [(18C6)$_2$Na$_2$(H$_2$O)$_2$]$_{1/2}$[Cd(SCN)$_3$] with tetragonal arrangements of infinite $[Cd(SCN)_3^-]_\infty$ chains

As portrayed in Figs. 3 and 4, in [(18C6)M][$Cd(SCN)_3$] where $M^+ = K^+$ (**1**), Na^+ (**2**), the anionic $[Cd(SCN)_3^-]$ complex form 1-D infinite zigzag chains [1a]. The infinite anionic $[Cd(SCN)_3^-]_\infty$ chains in **1** (Fig. 3) and **2** (Fig. 4) are arranged in an approximate tetragonal array, creating square channels which are filled by two monomeric $[(18C6)K]^+$ (in **1**) or by the dimeric $[(18C6)_2Na_2(H_2O)_2]^{2+}$ (in **2**) cations. Owing to the disk-like monomeric $[(18C6)K]^+$ cations in **1**, the infinite $[Cd(SCN)_3^-]_\infty$ zigzag chains align in a parallel manner, resulting in an acentric space group $Cmc2_1$. In contrast, the dimeric structure of the $[(18C6)_2Na_2(H_2O)_2]^{2+}$

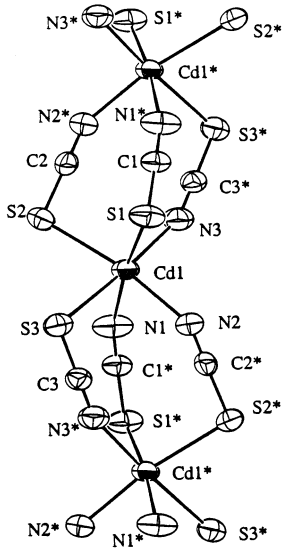

Fig. 2. Infinite 1-D anionic single chain of $[Cd(SCN)_3^-]_\infty$.

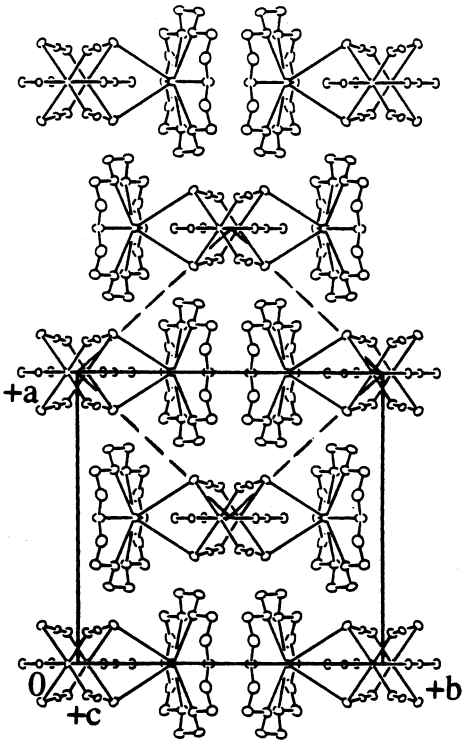

Fig. 3. Crystal packing of [(18C6)K][Cd(SCN)$_3$] (**1**) as viewed along the crystallographic c-axis depicting the approximately tetragonal arrangement of the zigzag $[Cd(SCN)_3^-]_\infty$ chains, creating square channels (dashed lines) which are filled with the disk-like $[(18C6)K]^+$ monocations.

dications in **2**, which reside on a crystallographic site symmetry of inversion center, cause the infinite $[Cd(SCN)_3^-]_\infty$ zigzag chains to align in an antiparallel fashion, resulting in a centrosymmetric space group $P2_1/n$. Fig. 5 depicts the parallel (a) and antiparallel (b) alignments of the infinite zigzag $[Cd(SCN)_3^-]_\infty$ chains in **1** and **2**, respectively (only Cd atoms are shown).

For the NLO application, **1**, with the noncentrosymmetric space group, gives rise to efficient second harmonic generation (SHG) effects (strong, phase-matchable, type A NLO crystals). With a centrosymmetric space group, **2** gives rise to no SHG effects. In this regard, the crown-ether–metal complex cations play the role of spacers/controllers, dictating the alignments of the zigzag $[Cd(SCN)_3^-]_\infty$ chains.

3.2. Hexagonal arrangements: structures of [(12C4)$_2$Na][Cd(SCN)$_3$] and [R$_4$N][Cd(SCN)$_3$] (R = Me and Et)

In order to investigate the effect of size and shape of the cation on the arrangement and alignment of the $[Cd(SCN)_3^-]_\infty$ chains, we synthesized $[(12C4)_2Na][Cd(SCN)_3$ (**3**) [1b] which has a smaller cationic crown-ether–metal

complex. Here the $[Cd(SCN)_3^-]_\infty$ chains are arranged in a hexagonal array, creating triangular channels which are filled by the sandwich $[(12C4)_2Na]^+$ cations, as shown in Fig. 6. The zigzag $[Cd(SCN)_3^-]_\infty$ chains in **3** are aligned in an antiparallel fashion owing to the symmetrical sandwich $[(12C4)_2Na]^+$ cations, thereby resulting in a centrosymmetric space group $P2_1/n$.

A detailed comparison of the structure **3** with that of [(18C6)K][$Cd(SCN)_3$] (**1**) and $[(18C6)_2Na_2(H_2O)_2]_{1/2}[Cd(SCN)_3]$ (**2**) revealed that the arrangement and the alignment of the infinite anionic $[Cd(SCN)_3^-]_\infty$ zigzag chains are dictated by the dimensions and symmetry, respectively, of the crown-ether–metal cations. From a crystal engineering point of view, depending upon the dimensions of the cations, the infinite anionic $[Cd(SCN)_3^-]_\infty$ chains could adopt either a tetragonal arrangement, creating the square channels which are filled with larger cations (as observed in both **1** and **2**) or a hexagonal arrangement, creating the triangular channels which are filled with the smaller cations (as observed in **3**). The relative alignment (either parallel or antiparallel) of the anionic chains, however, is determined by the symmetry (or approximate symmetry) of the cations. Thus, both the dimeric

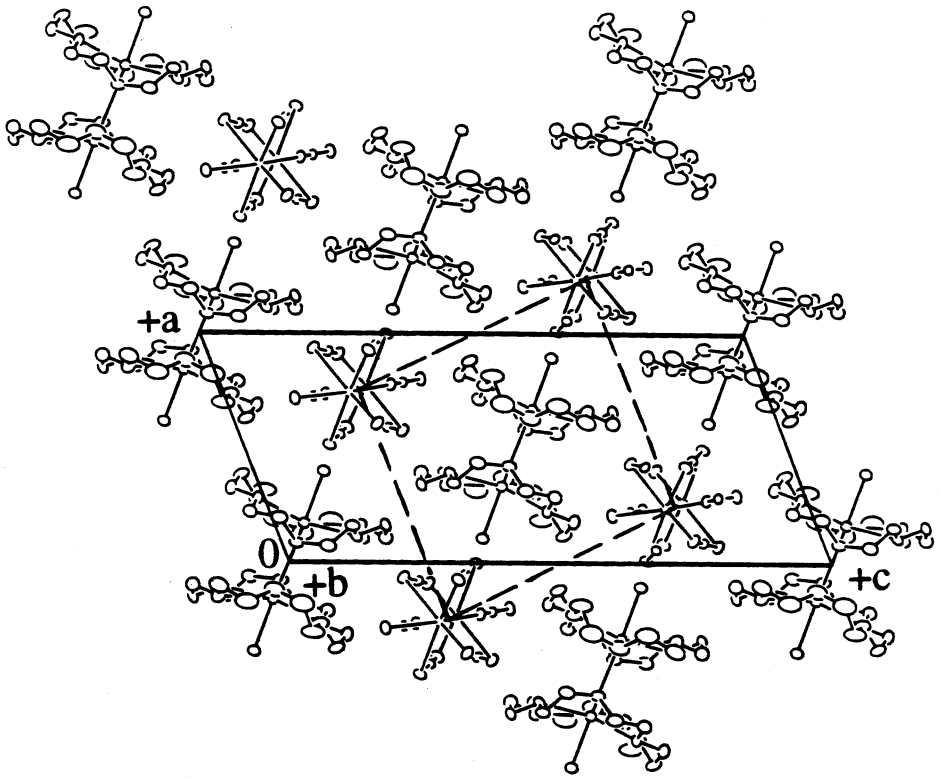

Fig. 4. Crystal packing of $[(18C6)_2Na_2(H_2O)_2]_{1/2}[Cd(SCN)_3]$ (**2**) as viewed along the crystallographic *b*-axis depicting the approximately tetragonal arrangement of the zigzag $[Cd(SCN)_3^-]_\infty$ chains, creating square channels (dashed lines) which are filled with the dimeric $[(18C6)_2Na_2(H_2O)_2]^{2+}$ dications.

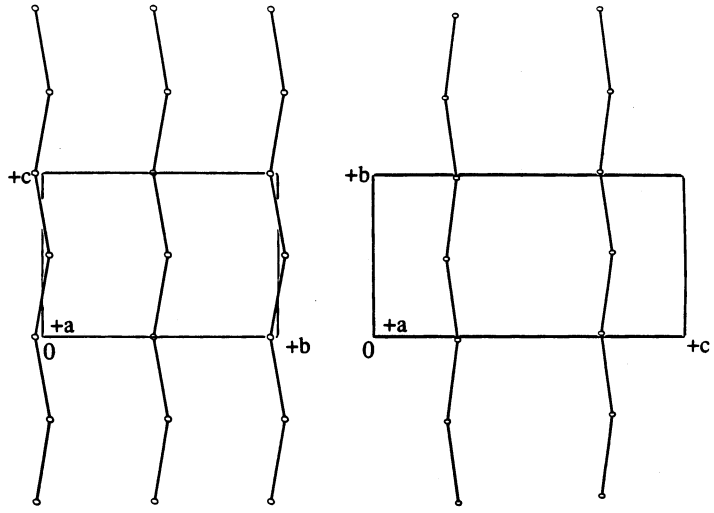

Fig. 5. The Cd atoms in **1** and **2** form infinite zigzag chains with Cd···Cd distances of 5.41 Å and Cd···Cd···Cd angles of 162° and with (left) parallel alignment in **1** and (right) antiparallel alignment in **2**.

dication in **2** and the sandwich monocation in **3** give rise to antiparallel alignment of the zigzag $[Cd(SCN)_3^-]_\infty$ chains with the centrosymmetric space groups ($P2_1/n$) whereas the disk-like cation in **1** gives rise to parallel alignment of the zigzag $[Cd(SCN)_3^-]_\infty$ chains with noncentrosymmetric space group ($Cmc2_1$) (the symmetry effect). We shall revisit the dimension and symmetry effects in a later section.

The dimension and symmetry effects can also be extended to cations of different sizes and shapes. For example, with relatively small, tetrahedral cations such as $(Me_4N)^+$ and $(Et_4N)^+$, the $[Cd(SCN)_3^-]_\infty$ chains are also arranged in an approximate hexagonal array with the cations occupying the triangular channels in both $[Me_4N][Cd(SCN)_3]$ (**4**) [10] and $[Et_4N][Cd(SCN)_3]$ (**5**) [11] (Fig. 5b) [5]. Though both the Me_4N^+ and the Et_4N^+ salts give rise to noncentrosymmetric space groups $Pna2_1$ and $Cmc2_1$, respectively, the $[Cd(SCN)_3^-]_\infty$ chains are aligned in an antiparallel (albeit approximately) and parallel fashions in **4** and **5**, respectively. As a consequence, the latter exhibits efficient second-order NLO effects [1e].

3.3. Other one-dimensional metal thiocyanate single-chain structures

Other types of 1-D metal thiocyanate chain structures are also known. Most of them, however, are neutral chains [12]. One interesting example of 1-D anionic metal thiocyanate chains is $[Me_4N]_2[Cd(SCN)_4]$ [10]. Here an infinite chain of $[Cd(SCN)_4^-]_\infty$ is formed wherein each Cd(II) ion is octahedrally coordinated with two *trans* N-bonded terminal NCS^- ligands and four bridging SCN^- ligands (2S and 2N, S *trans* to S and N *trans* to N) as depicted in Fig. 7. Apparently the *trans* influence is violated here. Topologically, this compound is related to

$[Me_4N][Cd(SCN)_3]$ [10] discussed earlier in the following sense. If each bridging SCN^- is conceptually visualized as a 'monoatomic' pseudohalide ligand, then the 1-D chains of $[Cd(SCN)_3^-]_\infty$ in $[Me_4N]_2[Cd(SCN)_4]$ may be considered as edge-sharing polyoctahedra of Cd(II) coordinations whereas the 1-D chains in $[Me_4N][Cd(SCN)_3]$ can be considered as face-sharing polyoctahedra of Cd(II) coordinations.

4. One-dimensional double-chain anionic cadmium-thiocyanate structures with cationic spacers/controllers: structures of $[(15C5)_2Na_2(H_2O)_2]_{1/2}[Cd_2(SCN)_5]$ and $[(15C5)_2K][Cd_2(SCN)_5]$

The first examples of double-chain $[Cd_2(SCN)_5^-]_\infty$ coordination solids are observed in $[(15C5)_2Na_2(H_2O)_2]_{1/2}[Cd_2(SCN)_5]$ (**6**) [1c] and $[(15C5)_2K][Cd_2(SCN)_5]$ (**7**)

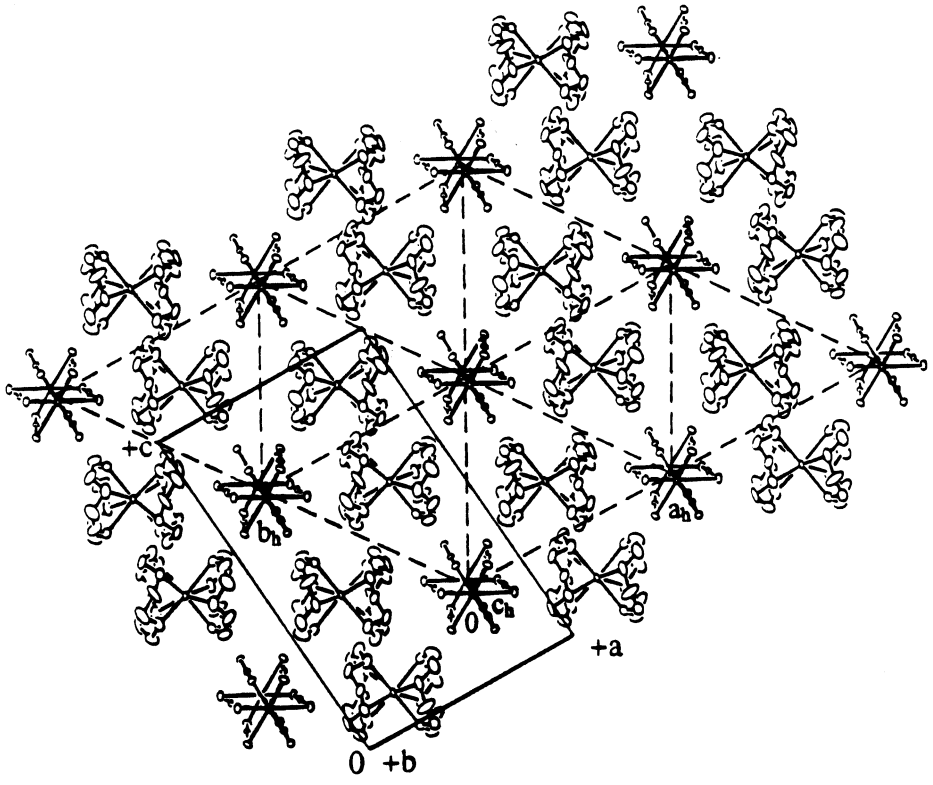

Fig. 6. Crystal packing of $[(12C4)_2Na][Cd(SCN)_3]$ (**3**) as viewed along the crystallographic *b*-axis depicting an approximately hexagonal arrangement of zigzag $[Cd(SCN)_3^-]_\infty$ chains, giving rise to triangular channels which are filled with the $[(12C4)_2Na]^+$ cations. The crystallographic monoclinic unit cell is indicated by *a*, *b*, and *c* (—) while the noncrystallographic pseudo hexagonal unit cell by a_h, b_h, and c_h (---).

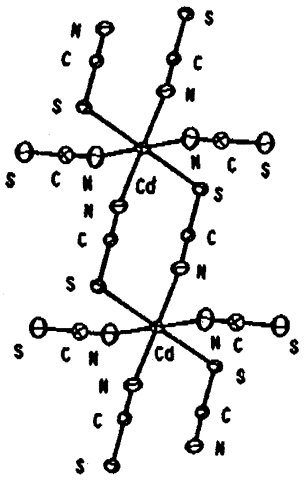

Fig. 7. The 1-D anionic $[Cd(SCN)_4^-]_\infty$ chain in $[Me_4N]_2[Cd(SCN)_4]$ [10] (adapted from Ref. [10]).

[1c] (Fig. 6) [1f]. In both structures, the infinite anionic cadmium-thiocyanate structures consist of 1-D polymeric chains with the building blocks of dicadmium-thiocyanate complex, $[Cd_2(SCN)_5^-]$, which may be referred to as double-chain structures, as portrayed in Fig. 8. Cd atoms are all octahedrally coordinated with 3N and 3S from four 'linkage' (type IIa, Chart 2) and two 'bridging' (type IIIa, Chart 2) SCN^- ligands while the S atom is *trans* to the N atom. The anionic 1-D double-chain $[Cd_2(SCN)_5^-]_\infty$ structures can be envisioned as two anionic 1-D single-chain $[Cd(SCN)_3^-]_\infty$ fused together via sharing of one bridging SCN^- ligands (per each pair of Cd atoms, one from each chain), giving rise to an infinite double chain of $[Cd_2(SCN)_5]^-$ with a Cd···Cd distance of 3.7 Å. Alternatively, it can also be considered as an infinite chain of edge-sharing bi-octahedral complexes $[Cd_2(SCN)_{10}]^{6-}$ sharing five SCN^- ligands, giving rise to the double chain of $[Cd_2(SCN)_{10/2}]^-$.

If viewed along the chain direction (Fig. 9), the arrangement of the double-chains $[Cd_2(SCN)_5^-]_\infty$ can be likened to a brick-layer pattern. From a crystal engineering point of view, the crown-ether–metal cations in **6** and **7** serve as both spacer and the controller for the arrangements and the alignments of the anionic double-chains, respectively. First, let us consider the spacer effect. The arrangement of the anionic double-chains $[Cd_2(SCN)_5^-]_\infty$ is affected by the dimensions of crown-ether–metal cations. With the large cations such as the dimeric $[(15C5)_2Na_2(H_2O)_2]^{2+}$ dications in **6**, the centers of the 'bricks' form a tetragonal array, creating square channels which are occupied by the the dimeric $[(15C5)_2Na_2(H_2O)_2]^{2+}$ dications whereas with the smaller cations such as the sandwich $[(15C5)_2K]^+$ monocations in **7**, the centers of the 'bricks' (the rectangular shape (end-on view) of the double-chains) form approximate hexagonal arrangement, creating triangular channels which are filled with the sandwich $[(15C5)_2K]^+$ monocations. The second effect is the controller effect. The double-chains in both **6** and **7** are aligned in an

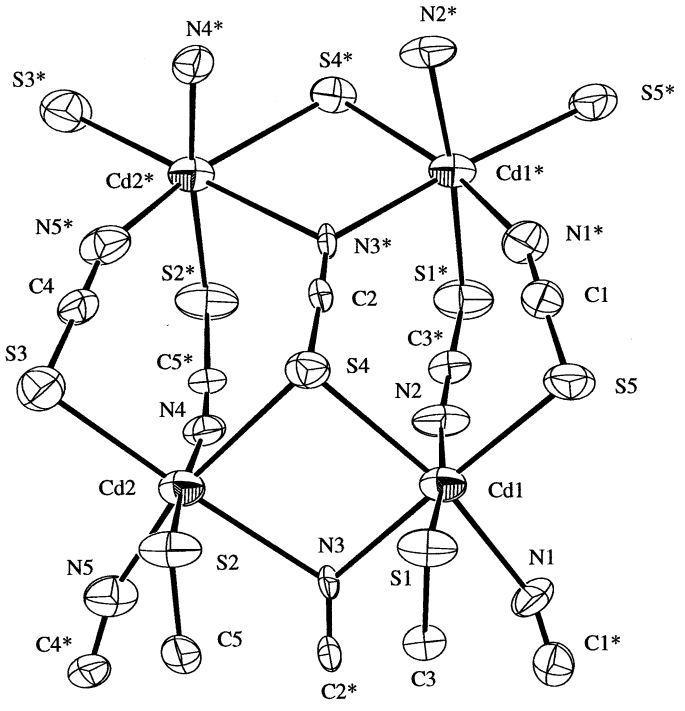

Fig. 8. The infinite 1-D anionic double-chain of $[Cd_2(SCN)_5^-]_\infty$ observed in $[(15C5)_2Na_2(H_2O)_2]_{1/2}$-$[Cd_2(SCN)_5]$ (**6**) and $[(15C5)_2K][Cd_2(SCN)_5]$ (**7**).

antiparallel fashion, owing to the symmetrical and spherical shapes of the dimeric (in **6**) and the sandwich (in **7**) crown-ether–metal cations. Finally, the symmetry of the crystal structure is also dictated by the symmetry (or approximate symmetry) of

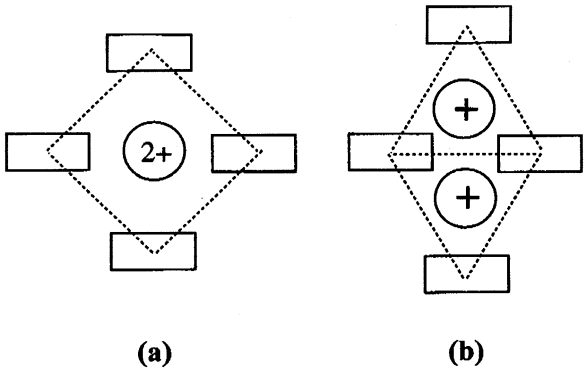

Fig. 9. The brick layer pattern (end-on view) of the spatial arrangement of the 1-D double chain $[Cd_2(SCN)_5^-]_\infty$ in **6** and **7**. The centers of the 'bricks' form (a) a tetragonal array, creating square channels housing the relatively large dimeric $[(15C5)_2Na_2(H_2O)_2]^{2+}$ dications in **6**; and (b) a rhombic (i.e. approximately hexagonal) arrangement, creating triangular channels housing the sandwich $[(15C5)_2K]^+$ monocations in **7**.

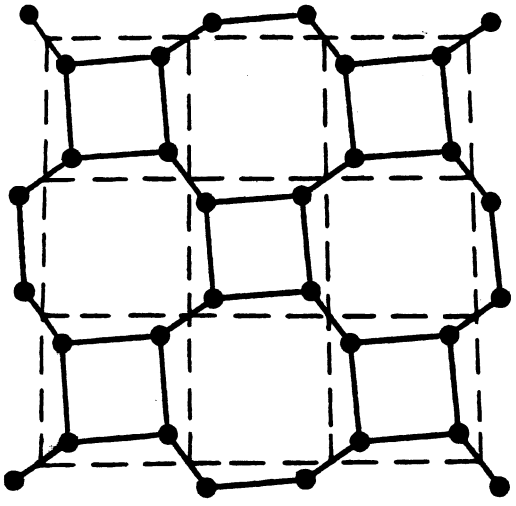

Fig. 10. Tetragonal array of dicadmium Cd_2 units arranged in a checkerboard pattern in the layered structure of $[(12C4)_2Cd][Cd_2(SCN)_6]$ (**8**) (note that the Cd atoms are not bonded and that $[(12C4)_2Cd]^{2+}$ and SCN^- ligands are omitted for clarity).

the cations. Thus, the centrosymmetric dimeric dication in **6** gives rise to the centrosymmetry space group $P2_1/c$ while the sandwich monocation in **7** results in a noncentrosymmetric space group $Pna2_1$. These effects will be discussed further in a later section.

5. Two-dimensional layered anionic cadmium-thiocyanate structures with cationic templates

To the best of our knowledge, there is only one previous example of 2-D anionic cadmium-thiocyanate layered structure, namely, $RbCd(SCN)_3$ [13], though layered structures are known for other mixed-metal thiocyanate compounds (e.g. $CoHg_2(SCN)_6 \cdot C_6H_6$) [14]. In the following sections, we shall describe the structures of two 2-D anionic cadmium-thiocyanate coordinate solids recently synthesized in our laboratory.

5.1. Dicadmium complexes as building blocks: structure of $[(12C4)_2Cd][Cd_2(SCN)_6]$

The first example of a novel 2-D cadmium-thiocyanate coordination solid within the IPOS series, formulated as $[(12C4)_2Cd][Cd_2(SCN)_6]$ (**8**) [2a,b], contains the sandwich $[(12C4)_2Cd]^{2+}$ dication and the anionic 2-D polymeric network of $[Cd_2(SCN)_6]^{2-}$. As depicted in Fig. 10, the Cd atoms in the $[Cd_2(SCN)_6^{2-}]_\infty$ layers are octahedrally coordinated with two N atoms from the 'bridging' NCS^- ligands

(type IIc, Chart 2) and two N atoms and two S atoms from the 'linkage' SCN^- groups (type IIa, Chart 2) as portrayed in Fig. 11.

The most important feature of the structure of **8** is the square net formed by the 'dangling' S atoms of the two bridging NCS^- groups within each $[Cd_2(NCS)_2]$ dimer, giving rise to a noncrystallographic, approximate square sublattice. These squares are in reality holes as portrayed in the space-filling model (Fig. 12a) of the square net of the 2-D structure of the anionic polymer $[Cd_2(SCN)_6^{2-}]_\infty$ with the $[(12C4)_2Cd]^{2+}$ dications removed. Half of these square holes (type A, hereafter referred to as 'deep' holes) are filled with the $[(12C4)_2Cd]^{2+}$ dications. The other half (type B, hereafter referred to as 'shallow' holes) are filled with two out-of-plane linkage SCN^- groups, arranged in an antiparallel fashion. The space-filling diagram of one layer of $[(12C4)_2Cd][Cd_2(SCN)_6]$ with the 'deep' holes (type A) filled with the $[(12C4)_2Cd]^{2+}$ dications is portrayed in Fig. 12(b). Here, the sulfur atoms of the 'bridging' NCS^- ligands are labeled to highlight the non-crystallographic square lattice and the square holes formed by these S atoms. The remaining space in these 'shallow' holes (type B) are occupied by the $[(12C4)_2Cd]^{2+}$ cations protruded from an adjacent layer. Within each layer, the 'deep' holes (type A) and the 'shallow' holes (type B) alternate like a 'checkerboard' as depicted schematically in Fig. 13 (left). The relative arrangement between the layers, however, is rather

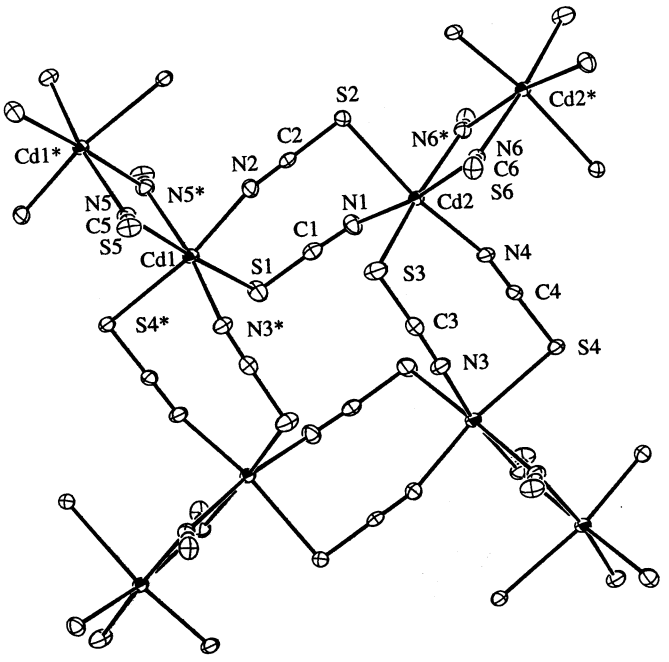

Fig. 11. ORTEP diagram of $[Cd_2(SCN)_6]^{2-}$ in **8**. The symmetry-related atoms are labeled with asterisks. Each Cd atom is octahedrally coordinated with *cis*-S_2N_4.

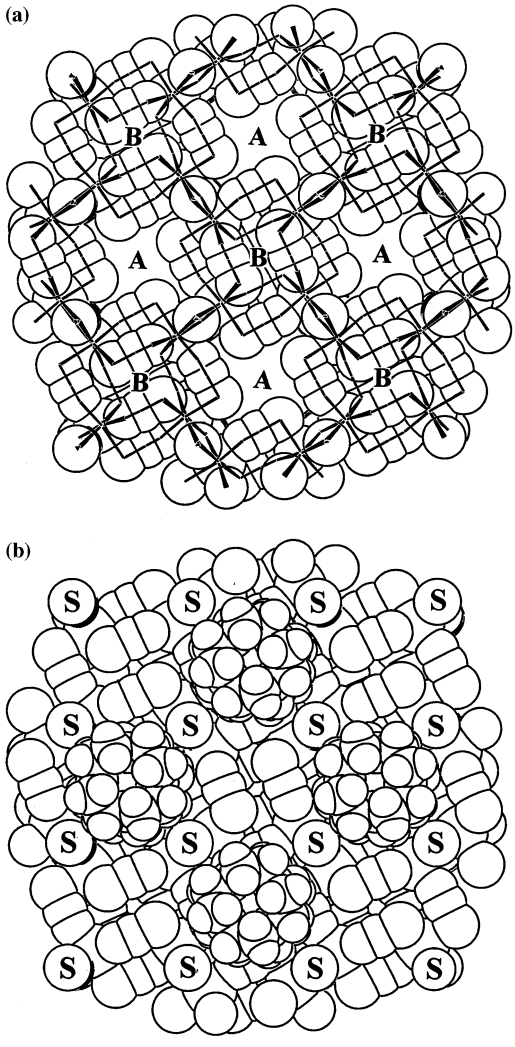

Fig. 12. Space-filling models of (a) the square net of the layered anionic polymer $[Cd_2(SCN)_6^{2-}]_\infty$ with the $[(12C4)_2Cd]^{2+}$ cations removed to expose the 'deep' (A) and 'shallow' (B) square holes in $[(12C4)_2Cd][Cd_2(SCN)_6]$ (**1**); (b) one layer with the 'deep' holes (type A) filled with the$[(12C4)_2Cd]^{2+}$ dications. The sulfur atoms of the 'bridging' NCS^- ligands are labeled to highlight the noncrystallographic square lattice (and the square holes) formed by these 'dangling' S atoms.

interesting. As a result of the crystallographic C-centering, the adjacent layers complement one another with the 'deep' holes of one layer being aligned with the 'shallow' holes of an adjacent layer (see Fig. 13 (right)). In this context, the structure may be likened to stacks of 'eggs in cartons' with the $[(12C4)_2Cd]^{2+}$ dications as 'eggs' and the tetragonal nets of the polymeric $[Cd_2(SCN)_6^{2-}]_\infty$ layers as 'cartons'. The $[(12C4)_2Cd]^{2+}$ dications fit snugly into the complementary 'deep'

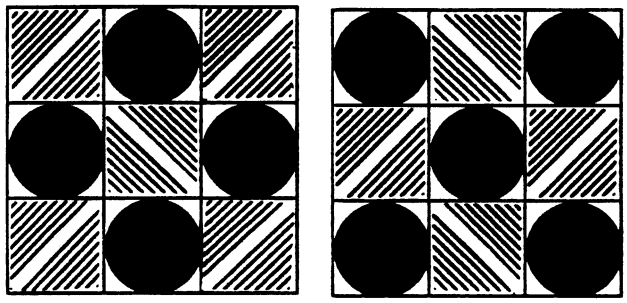

Fig. 13. Schematic 'checker board' representations of adjacent layers of $[(12C4)_2Cd][Cd_2(SCN)_6]$ (**8**). The 'deep' (type A) and 'shallow' (type B) holes are represented by white and shaded boxes, respectively. The $[(12C4)_2Cd]^{2+}$ dications are denoted by black circles. The stripes in the shaded boxes illustrate schematically the 'herringbone' arrangement of the antiparallel 'linkage' SCN^{2-} ligands. The left figure corresponds to the space-filling model in Fig. 12. Note that the layers alternate and complement one another such that the $[(12C4)_2Cd]^{2+}$ dications in the 'deep' holes of one layer protrude into the 'shallow' holes of the adjacent layer (see text).

and 'shallow' holes of adjacent layers. As we shall see later, this tight fit is an indication that the square motif of the anionic $[Cd_2(SCN)_6^{2-}]_\infty$ polymeric layers may be induced by the square shape of the $[(12C4)_2Cd]^{2+}$ dications.

5.2. Tricadmium complexes as building blocks: structure of $[(12C4)_2Cd][Cd_3(SCN)_8]$

The second example of 2-D cadmium-thiocyanate coordination solid, formulated

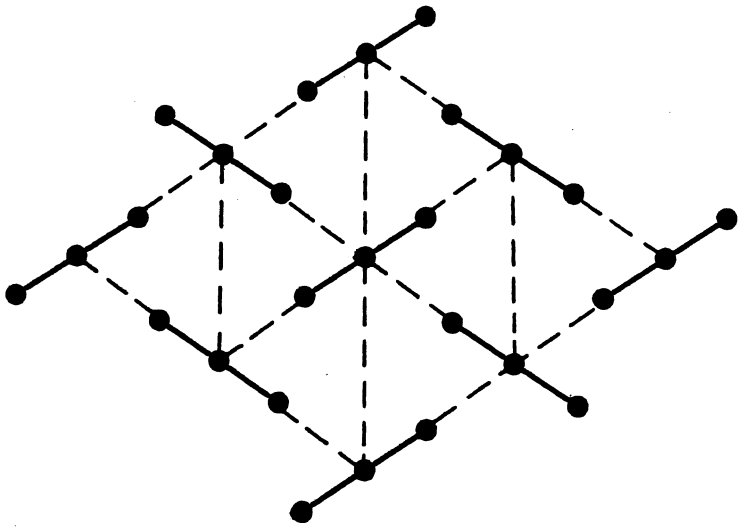

Fig. 14. Hexagonal array of linear tricadmium Cd_3 units arranged in a herringbone pattern in the layered structure of $[(12C4)_2Cd][Cd_3(SCN)_8]$ (**9**) (note that the Cd atoms are not bonded and that $[(12C4)_2Cd]^{2+}$ and SCN^- ligands are omitted for clarity).

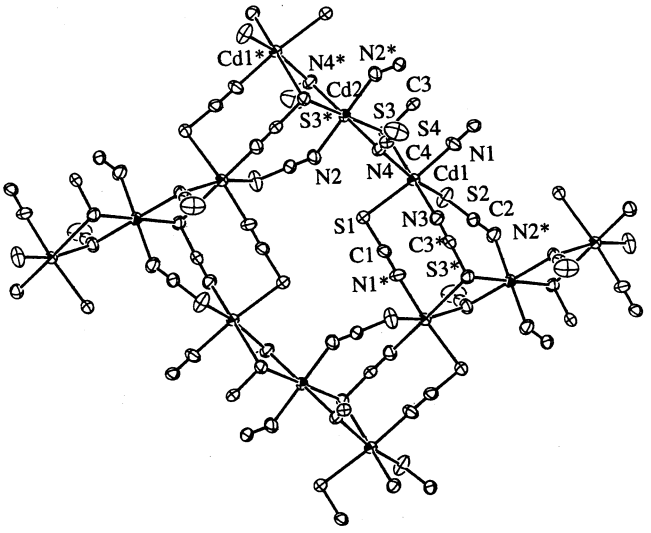

Fig. 15. ORTEP diagram of $[Cd_3(SCN)_8]^{2-}$ (**9**). The symmetry-related atoms are labeled with asterisks. The central Cd2 atoms are octahedrally coordinated with *trans*-S_2N_4 atoms while the end Cd1 atoms are octahedrally coordinated with *fac*-S_3N_3 atoms.

as $[(12C4)_2Cd][Cd_3(SCN)_8]$ (**9**) [2b], has a structure consisting of hexagonal array of linear trimeric Cd_3 units arranged in herringbone pattern with the $[Cd_3(SCN)_8]^{2-}$ complex as the building block as depicted in Fig. 14.

As portrayed in Fig. 15, there are two crystallographically independent cadmium atoms in the $[Cd_3(SCN)_8]^{2-}$ unit: the central cadmium, Cd2, is located at an inversion center while the end ones, Cd1 and Cd1*, are related by the same inversion symmetry. Cd1 is octahedrally coordinated with three S and three N atoms whereas Cd2 is octahedrally coordinated with two S and four N atoms.

There are four crystallographically independent SCN^- ligands, exhibiting distinctively different bridging modes as portrayed in Fig. 15. Adopting the terminology used in previous section, S(n)C(n)N(n) ligands where $n = 1, 2, 3$, may be termed 'linkage' thiocyanates whereas S4C4N4 may be described as 'bridging' (through N4) thiocyanate ligand (type IIc, Chart 2) with a dangling sulfur atom (S4). The three linkage SCN^- in **9** can be categorized into two types: S1C1N1 and S2C2N2 bridge two Cd atoms via the N and the S atoms (type IIa, Chart 2) whereas S3C3N3 bridges three Cd atoms with the S atom coordinating to two Cd atoms and the N atom coordinating to one Cd atom (type IIIa, Chart 2).

The space-filling model of **9** is portrayed in Fig. 16(a,b), with and without the $[(12C4)_2Cd]^{2+}$ dications, respectively. It can be seen that the 'dangling' sulfur atoms (labeled as S) of the 'bridging' S4C4N4 ligands form a highly distorted hexagonal net of approximate dimensions $a_s = a_h/2$, $b_s = b_h/2$, and $c_s = c_h$, giving rise to highly distorted triangular holes. Employing the same terminology used in

the description of the structure of **8**, half of these triangular holes, which are filled with the $[(12C4)_2Cd]^{2+}$ dications, may be termed the 'deep' (type A) holes. The other half, which are filled by the out-of-plane linkage S3C3N3 ligands, may be termed the 'shallow' (type B) holes. The 'deep' and 'shallow' holes alternate within the same layer, as shown in Fig. 16(a). If we take into account the adjacent layers, the 'deep' and 'shallow' holes turn into highly distorted 'octahedral' (type A) and 'tetrahedral' (type B) holes, respectively, as depicted in the idealized schematic

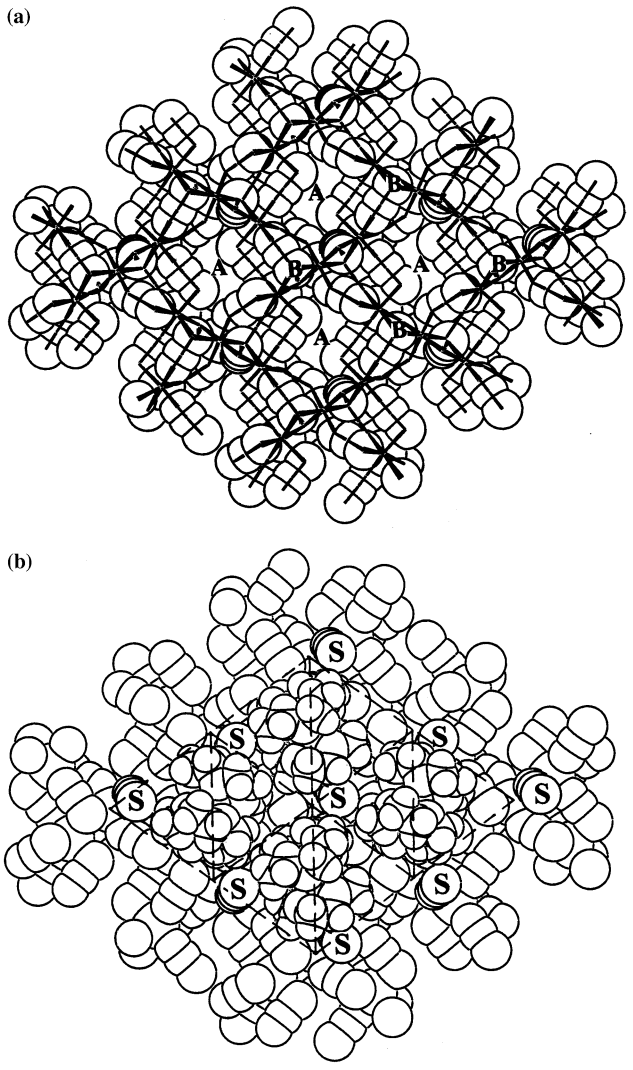

Fig. 16. Space-filling diagram of one layer of $[(12C4)_2Cd][Cd_3(SCN)_8]$ (**9**): (a) with the$[(12C4)_2Cd]^{2+}$ cations removed to expose the 'deep' (type A) and 'shallow' (type B) holes; and (b) with the $[(12C4)_2Cd]^{2+}$ dications. In (b) the sulfur atoms of the 'bridging' (N4C4S4) ligands are labeled to highlight the highly distorted hexagonal net and the triangular holes formed by these S atoms.

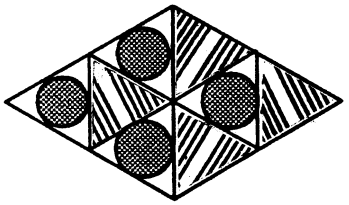

Fig. 17. Schematic representation of one layer of the approximate hexagonal net of the 'dangling' sulfur atoms (labeled with S in Fig. 16b) of the $[Cd_3(SCN)_8^{2-}]$ layers in **9**. An approximately hexagonal closed-packed (hcp) arrangement of the adjacent sulfur layers creates highly distorted octahedral holes (open triangles) which house the $[(12C4)_2Cd]^{2+}$ sandwich dications (solid circles) and tetrahedral holes which are filled with the out-of-plane linkage SCN^- ligands (striped triangles). Note that the 'octahedral' and 'tetrahedral' holes correspond to the 'deep' (type A) and 'shallow' (type B) holes of individual layers shown in Fig. 16(a). The stripes in the shaded triangles illustrate schematically the orientation of the out-of-plane linkage thiocyanate ligands.

representation in Fig. 17. The six dangling sulfurs, three from each neighboring layers (only one layer is shown), form 'octahedral' (type A, open triangles) holes which encapsulate the $[(12C4)_2Cd]^{2+}$ dications (solid circles) with extensive hydrogen bonding. The 'tetrahedral' (type B, striped triangles) holes, formed by four dangling sulfurs, three from one layer and one from an adjacent layer, are filled with the out-of-plane linkage SCN^- (labeled 3) ligands. In this regard, the arrangement of the dangling sulfur atoms may be likened to hexagonal closed packing of spheres, producing one large octahedral hole and two smaller tetrahedral holes per sphere.

A detailed comparison of the structures of **8** and **9** revealed that while the $[(12C4)_2Cd]^{2+}$ dications in **8** are oriented in the 'upright' position, the $[(12C4)_2Cd]^{2+}$ dications in **9** are lying almost 'sideways' with respect to the $[Cd_3(SCN)_8^{2-}]_\infty$ layers

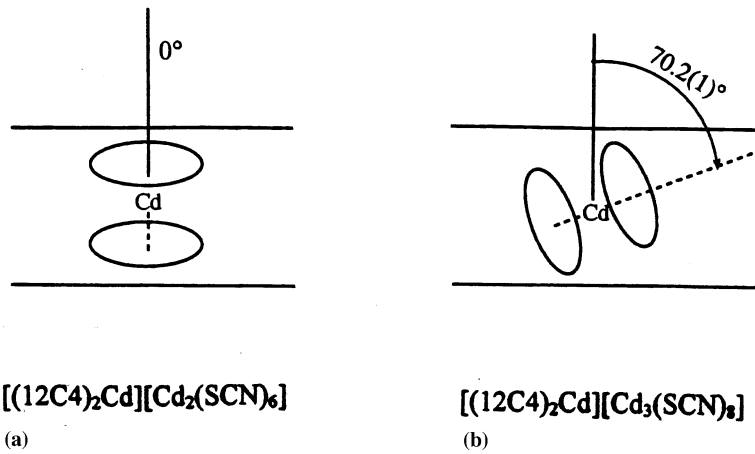

Fig. 18. Schematic representation of the relative orientations of the $[(12C4)_2Cd]^{2+}$ dications with respect to the cadmium-thiocyanate layers: (a) 'upright' (0°) in **8**; and (b) approximate 'sideways' (70.2(1)°) in **9**.

as depicted schematically in Fig. 18. More precisely, the 12C4 ligands of the $[(12C4)_2Cd]^{2+}$ dications make an angles of 0° (upright) and 70.2(1)° (sideways) with respect to the anionic cadmium-thiocyanate layers (as represented by the least-square plane passing through the cadmium atoms). This effect may be called 'anisotropic templating' [33]. We shall revisit this effect in a later discussion.

5.3. Other two-dimensional metal thiocyanate structures

Though layered transition-metal thiocyanate structures are rather rare, we should mention two such compounds, $RbCd(SCN)_3$ [13] and $CoHg_2(SCN)_6 \cdot C_6H_6$ [14]. Each of these compounds adopt a unique layered structure distinctly different from the structures described above. For example, a different type of 2-D polymeric structure was observed for $RbCd(SCN)_3$ [13] in which octahedral $Cd(SCN)_4(NCS)_2$ and $Cd(NCS)_4(SCN)_2$ groups are connected by Cd–SCN–Cd bridges to form layers with Rb^+ ions residing in between the layers as depicted schematically in Fig. 19(a). Yet another example is the highly interesting tetragonal net found in $CoHg_2(SCN)_6 \cdot C_6H_6$ [14] where $Co(NCS)_6$ groups are linked through S atoms by pairs of Hg atoms which are themselves bridged by two S atoms of two SCN^- ligands. The resulting layers are intercalated with benzene molecules. This structure can be rationalized in terms of the hard–soft acid–base concept. Thus, Co, being a hard acid, is octahedrally coordinated with six hard base N atoms whereas the Hg, being a soft base, is tetrahedrally coordinated with four soft base S atoms.

6. Three-dimensional metal-thiocyanate structures

3-D anionic cadmium-thiocyanate structures are rare. Most known metal thiocyanate compounds with 3-D structures contain other metals or a combination of metals. We shall describe a few examples here.

6.1. Structure of $CsCd(SCN)_3$

The structure of $CsCd(SCN)_3$ [13] consists of the S-bonded octahedral complexes $Cd(SCN)_6$ and N-bonded octahedral complexes $Cd(NCS)_6$ connected by Cd–SCN–Cd bridges to form a perovskite-like 3-D framework as depicted schematically in Fig. 19(b).

6.2. Structures of $M(SCN)_2$ where $M = Zn$, Cd, Hg

The zinc in $Zn(SCN)_2$ [34a] has a coordination number of 4, consisting of the tetrahedral structural units ZnN_4 and ZnS_4 bridged by the Zn–SCN–Zn moiety (type IIa, Chart 2). The cadmium in $Cd(SCN)_2$ [34b] is hexacoordinated via 4S and 2N and having bridging type $(Cd-)_2SCN-Cd$ (type IIIa, Chart 2). The mercury in $Hg(SCN)_2$ [34c] is likewise hexacoordinated (2S + 4N). However, since the bond lengths of Hg···N (2.81 Å) exceed the Cd–N distance by 0.5 Å, with nearly equal

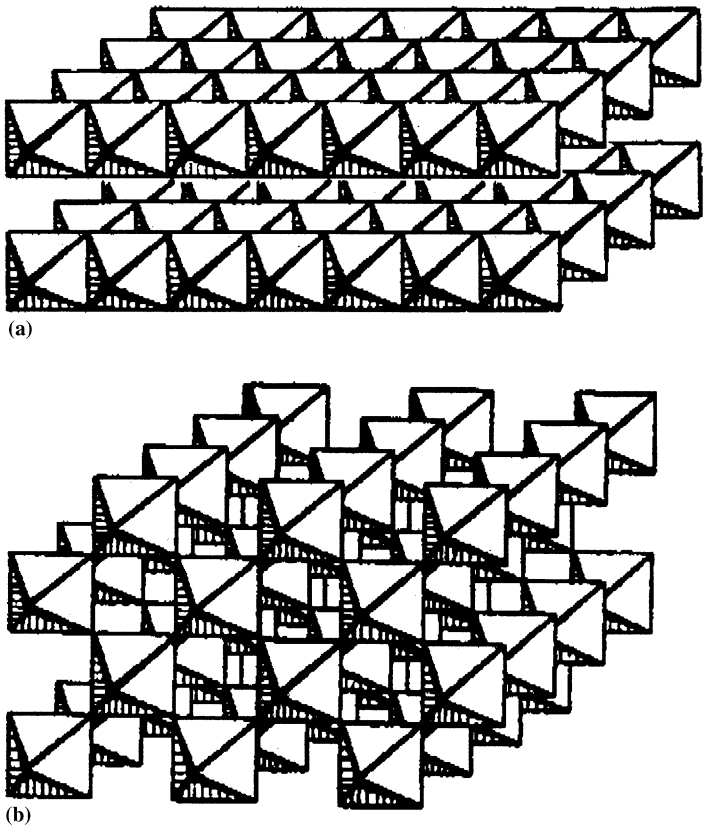

Fig. 19. Schematic representations of (a) a 2-D structure of $RbCd(SCN)_3$ depicting the $Cd(SCN)_4(NCS)_2$ and $Cd(NCS)_4(SCN)_2$ octahedra connected by Cd–SCN–Cd bridges to form layers with Rb^+ ions residing in between the layers; and (b) a 3-D structure of $CsCd(SCN)_3$ consisting of S-bonded $Cd(SCN)_6$ and N-bonded $Cd(NCS)_6$ octahedra connected by Cd–SCN–Cd bridges to form a perovskite-like framework (adapted from Ref. [13]).

atomic and ionic radii of Hg and Cd, $Hg(SCN)_2$ can be considered a linear molecule with the mercury having the coordination number of 2.

6.3. Structures of $MHg(SCN)_4$ (M = Mn, Fe, Co or Ni, Cu, Cd)

As further examples of 3-D structures, we shall discuss compounds of the type $MHg(SCN)_4$ (M = Mn, Fe, Co or Ni, Cu, Cd). In these complexes, mercury is usually tetrahedrally S-coordinated, while the ion of the other metal may be surrounded by four or six ligands. For instance, Co(II) has a tetrahedral N-coordination in $CoHg(SCN)_4$ [35] while Cu(II) has an octahedral coordination in $CuHg(SCN)_4$ [36] with N_4S_2 chromophores. The coordination modes of $CoHg(SCN)_4$ can be rationalized in terms of the hard–soft acid–base concept. Thus,

Co(II) ion, being a hard acid, is tetrahedrally coordinated by the hard base, the N atom of the bridging SCN^- ligands whereas the Hg(II) ion, being a soft acid, is bonded by the soft base, the S atom of the bridging SCN^- ligands. The coordination number 6 is, however, realized in compounds of the type $CoHg(SCN)_4 \cdot 2L$ (L = THF, py, or $PhNH_2$), where the Co(II) increases its coordination number to 6 by means of the donor molecules of the organic ligands [37].

As in $CoHg(SCN)_4$, the –SCN– ligands (type IIa, Chart 2) in $CdHg(SCN)_4$ [38] bridge the tetrahedrally coordinated N-bonded Cd atoms and the tetrahedrally coordinated S-bonded Hg atoms into a diamond-like 3-D network with space group $I\bar{4}$. As we shall discuss later for [(18C6)K][$Cd(SCN)_3$] (**1**) and related compounds, $CdHg(SCN)_4$ exhibits high hyperpolarizability due to the extended π-conjugation of the Cd–NCS–Hg bridges and their parallel alignments (along the crystallographic -4 axis) in the 3-D crystal structure. Indeed, it has been postulated [39] that the 3-D network provides the crystal with a larger domain for polarizability which in turn induces a larger macroscopic nonlinearity than that of the sum of individual dipolar SCN and octupolar CdN_4 and HgS_4 moieties. Efficient blue-violet (404.5 nm) light output by frequency doubling of a 809 nm GaAlAs diode laser has been demonstrated [34b] and shown to be phase matchable (type I from 0.74 to 1.12 μm and type II from 0.78 to 1.08 μm).

7. From molecular engineering to crystal engineering

7.1. Design criteria for nonlinear optical materials

We shall now consider the design criteria and the novel features of the IPOS systems as NLO materials [5–7]. The design of new materials may be conceptually divided into two steps: molecular engineering wherein the electronic properties of the molecule are optimized and crystal engineering wherein crystallization in certain symmetry pattern is achieved [15–21]. For organic NLO materials [7], the commonly adopted molecular design rules are (1) highly delocalized, easily polarizable system; and (2) large asymmetry in electronic distribution caused by intramolecular donor–acceptor charge transfer while crystal engineering requires the arrangement of the molecules in a noncentrosymmetric space group. The main problem, however, is that these two steps are generally not independent of one another. For instance, an organic compound whose molecular structure has been optimized for NLO properties by including a delocalized π-system with donor (push)–acceptor (pull) groups on both ends to achieve a high hyperpolarizability, as exemplified by $H_2N–C_6H_4–C_6H_4–NO_2$, tends to couple head-to-tail in crystal packing, resulting in a centrosymmetric space group, thereby nullifying the SHG effect [40,41]. Different counterions, however, can be used to avoid the formation of centric crystals. Such strategies have been successfully employed by Meredith, Marder, Cheng, Marks, respects, are different in many others. First, the role of the 'host' matrix and the 'guest' spacer/controller are reversed. While these researchers used organic host

with inorganic counterions, we use inorganic host and organic counterions. Second, while their NLO responses stem from the organic host, the NLO effects of our IPOS system are due to the inorganic component. Third, the organic NLO used in their studies are molecular donor–acceptor charge-transfer compounds, whereas the inorganic NLO components of our IPOS system are polymeric metal–ligand complexes. Yet another strategy in combining polarizable organic cations (Cat^+) and inorganic anions in crystal engineering of NLO crystals (as in $(Cat)H_2PO_4$) has been advocated by Zyss, Masse, and coworkers [42].

We note that the crown-ether–alkali-metal cadmium-thiocyanate coordination solid series satisfies all four 'molecular design' criteria for organometallic NLO compounds advocated by Kanis et al. [6a]. The four criteria for organometallic NLO compounds are (1) highly polarizable ligand π system, (2) easily polarizable (i.e. weakly bound valence electrons) metal atoms, (3) asymmetric metal coordination so as to give rise to an asymmetric electronic distribution at the metal center (the 'ideal' ligand environment being the arrangement of 'hard' and 'soft' ligands *trans* to one another), and (4) intense low-energy MLCT bands. The corresponding terms in our IPOS system are: (1) the SCN^- ligand has a polarizable π system, (2) the Cd^{2+} ion has a closed-shell d^{10} configuration which is highly polarizable, (3) the hard nitrogen and the soft sulfur ligands are *trans* to one another, and (4) the metal-to-ligand charge-transfer (MLCT) transition can be easily achieved due to low-lying π* orbitals of the ligand. In fact, $[(18C6)K][Cd(SCN)_3]$ (**1**) [1a] has been shown to exhibit efficient second-order NLO property [42] via the Kurtz–Perry powder technique [43]. Other 1-D anionic Cd–SCN coordination solids known so far to exhibit SHG effects are summarized in Table 1. In this and the related compounds, an intense MLCT band (or metal-mediated ligand $\pi \rightarrow \pi^*$ transition) has been observed at 220nm (with a shoulder at 262nm) in the solid-state electronic spectrum of the polymeric metal–thiocyanate system. Such a transition is believed to be the origin of the NLO responses.

7.2. Design strategies: symmetry control

General design strategies, in terms of symmetry control, as well as molecular and crystal engineering, in terms of electronic and stereochemical controls, have been formulated and will be discussed in this and the following sections. Specifically, for molecular engineering, symmetric coordinations around the metal should be avoided whereas for crystal engineering, symmetric countercations should not be used in the crystal packing, as illustrated in Chart 6. Here A_m and A_s refer to molecular and crystal engineering, respectively. The multiplication table is shown in Chart 7 (assuming $S = 0$ and $A = 1$). Details on the manipulation of S_m, A_m, S_c, and A_c will be discussed in the next section. The underlying principle is to avoid or eliminate electronic and stereochemical factors that tend to give rise to centric crystals.

Table 1
Molecular and crystal engineering of 1-D anionic cadmium-thiocyanate polymers with (crown-ether)–(alkali-metal) cations as spacers/controllers

Molecular engineering		Crystal engineering				SHG[a]
$[H–G]^{q+}$	$[M–L]^{q-}$	Spatial arrangement	Channel	Chain alignment	Crystal symmetry	
$[(18C6)K]^{+}$ disk (a)	$[Cd(SCN)_3]^{-}$	Tetragonal	□	Parallel <<	$Cmc2_1$	Yes
$[DB24C8)Na]^{+}$ coiled (c)	$[Cd(SCN)_3]^{-}$	Hexagonal	△	Parallel <<	Cc	Yes
$[(18C6)_2Na_2(H_2O)_2]^{2+}$ dimer (e)	$[Cd(SCN)_3]^{-}$	Tetragonal	□	Antiparallel <>	$P2_1/n$	No
$[(12C4)_2Na]^{+}$ sandwich (f)	$[Cd(SCN)_3]^{-}$	Hexagonal	△	Antiparallel <>	$P2_1/n$	No
$[(15C5)_2K]^{+}$ sandwich (f)	$[Cd_2(SCN)_5]^{-}$	Hexagonal	△	Antiparallel ≪≫	$Pna2_1$	Weak
$[(15C5)_2Na_2(H_2O)_2]^{2+}$ dimer (d)	$[Cd_2(SCN)_5]^{-}$	Tetragonal	□	Antiparallel ≪≫	$P2_1/c$	No

[a] Power measurement using the Kurtz–Perry technique.

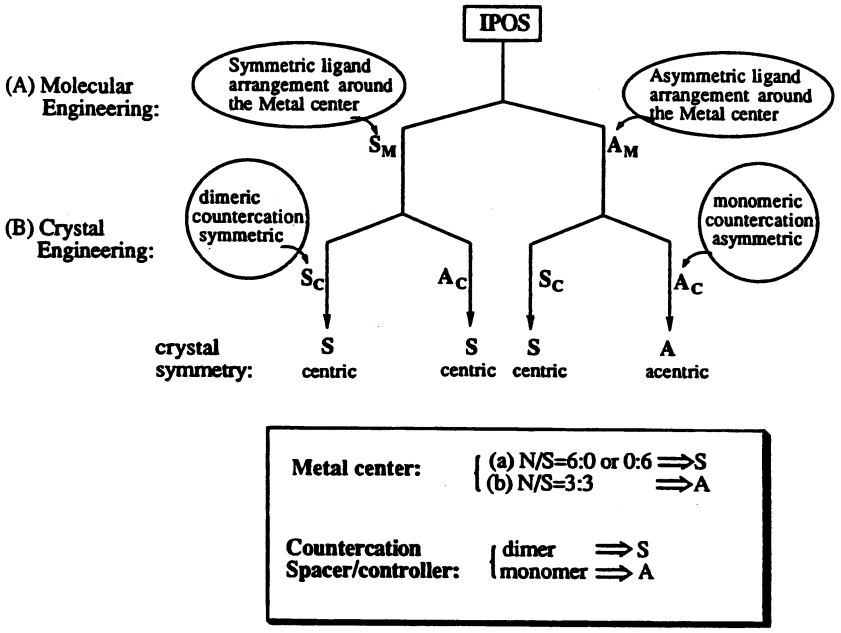

Chart 6. Separate but concomitant controls in molecular and crystal engineering.

We shall now discuss the various aspects of molecular design and crystal engineering.

7.3. From molecular to crystal engineering

The IPOS system, as exemplified by the series of structures discussed in this review, allows concomitant but independent molecular and crystal engineering in two separate controls, as illustrated in Chart 6. This feature is particularly useful in the tailoring of desirable materials and in the optimization of their properties. Intuitively, we should have several levels of electronic and stereochemical controls over the molecular and crystal symmetries.

c \ m	S_m	A_m
S_c	S	S
A_c	S	A

Chart 7. Multiplication table.

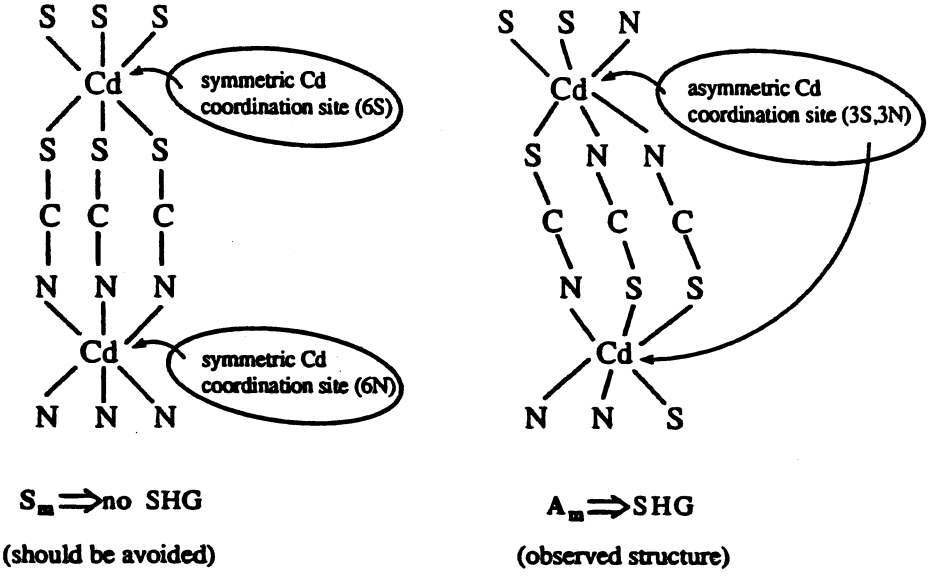

Chart 8. Molecular engineering. Left: symmetrical ligand arrangements of 6S or 6N should be avoided. Right: assymmetrical ligant arrangements of 3S and 3N gives rise to NLO (SHG) properties.

7.3.1. Molecular engineering: inorganic polymers (IP)

We have chosen ligands such as SCN^- because of their high degree of polarizability which is crucial in the development of their NLO properties. Furthermore, the ambidentate SCN^- ligand, with a hard N atom and a softer S atoms as donor atoms, tends to form polymeric structures with transition metal ions such as Cd^{2+}. At the molecular engineering level, the formation of symmetric Cd coordination site (S_m) such as 6N or 6S (Chart 8, left), however, should be avoided as it would inevitably lead to centrosymmetric crystal.

For the 1-D cadmium-thiocyanate system, the ideal arrangements are 3S and 3N around each Cd^{2+} ion with the S atoms *trans* to the N atoms (one observed example is depicted in Chart 8, right). The asymmetric arrangements of S and N atoms around the Cd atom give rise to asymmetrical Cd coordination (A_m) and hence highly asymmetric electronic distribution about the Cd atom. Other asymmetric arrangements with 2S and 4N or 4S and 2N (not shown) in the cadmium coordination sphere are also possible.

7.3.2. Crystal engineering: organic spacers/controllers (OS)

The crystal structures of the IPOS series are, to a large extent, controlled by the cationic host–guest complexes. We shall illustrate the crystal engineering principles with the 1-D single-chain systems. For example, the monomeric $[(18C6)K]^+$ cations in $[(18C6)K][Cd(SCN)_3]$ cause the anionic infinite $[Cd(SCN)_3^-]_\infty$ zigzag chains to be parallel, resulting in an acentric space group and efficient SHG effects. In contrast, the centrosymmetric dimeric $[(18C6)_2Na_2(H_2O)_2]^{2+}$ dications in

$[(18C6)_2Na_2(H_2O)_2]_{1/2}[Cd(SCN)_3]$ cause the $[Cd(SCN)_3^-]_\infty$ zigzag chains to align in an antiparallel fashion, resulting in a centric space group and hence the disappearance of the SHG effects. We therefore conclude that the host–guest cations play the role of organic spacers/controllers, dictating the arrangement of the $[Cd(SCN)_3^-]_\infty$ zigzag chains. We shall discuss in detail the general structural principles and crystal engineering of the IPOS systems in the next section.

8. Crystal engineering: dimension (size and shape), symmetry, and template effects

Table 1 summarizes the results of crystal engineering for 1-D single-chain $[Cd(SCN)_3^-]_\infty$ and double-chain $[Cd_2(SCN)_5^-]_\infty$ coordination solids with crown-ether–alkali-metal cations. The same results are represented diagramatically in Chart 10. We shall discuss each of the dominant effects—the geometry, symmetry, and template effects—in the following sections.

8.1. Cations as spacers (dimension effect)

The arrangement of the 1-D anionic $[Cd(SCN)_3^-]_\infty$ chains is to a significant extent dictated by the size and shape of the cations as exemplified by $[(18C6)_2Na_2(H_2O)_2]_{1/2}[Cd(SCN)_3]$ (**2**) and $[(12C4)_2Na][Cd(SCN)_3]$ (**3**) shown schematically in Chart 9. In other words, the cations serve as spacers, filling in the voids between the chains. With large spheroidal shaped cations such as the dimeric $[(18C6)_2Na_2(H_2O)_2]^{2+}$ in **2** (Fig. 4), tetragonal (or square) arrangement of the anionic $[Cd(SCN)_3^-]_\infty$ chains is favored. With small cations such as $[(12C4)_2Na]^+$ in **3** (Fig. 6), distorted hexagonal arrangement of the anionic $[Cd(SCN)_3^-]_\infty$ chains is observed. The approximate hexagonal arrangement of the $[Cd(SCN)_3^-]_\infty$ chains in $[(12C4)_2Na][Cd(SCN)_3]$ (**3**) can be conceptually derived from the approximate tetragonal motif in $[(18C6)_2Na_2(H_2O)_2]_{1/2}[Cd(SCN)_3]$ (**2**) by a formal distortion as illustrated schematically in Chart 9. Each square channel becomes two triangular channels. Note that the two $[(12C4)_2Na]^+$ monocations housed in two adjacent

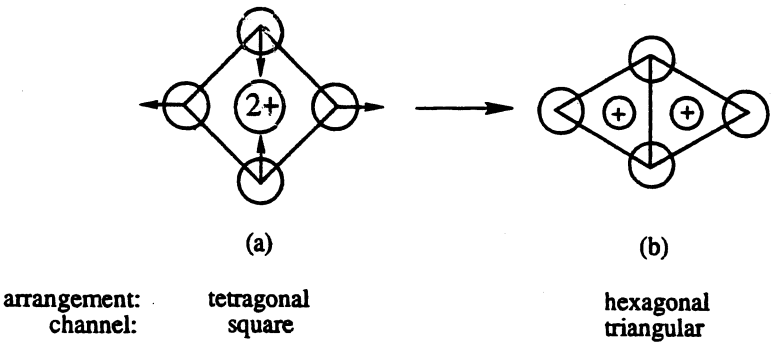

Chart 9.

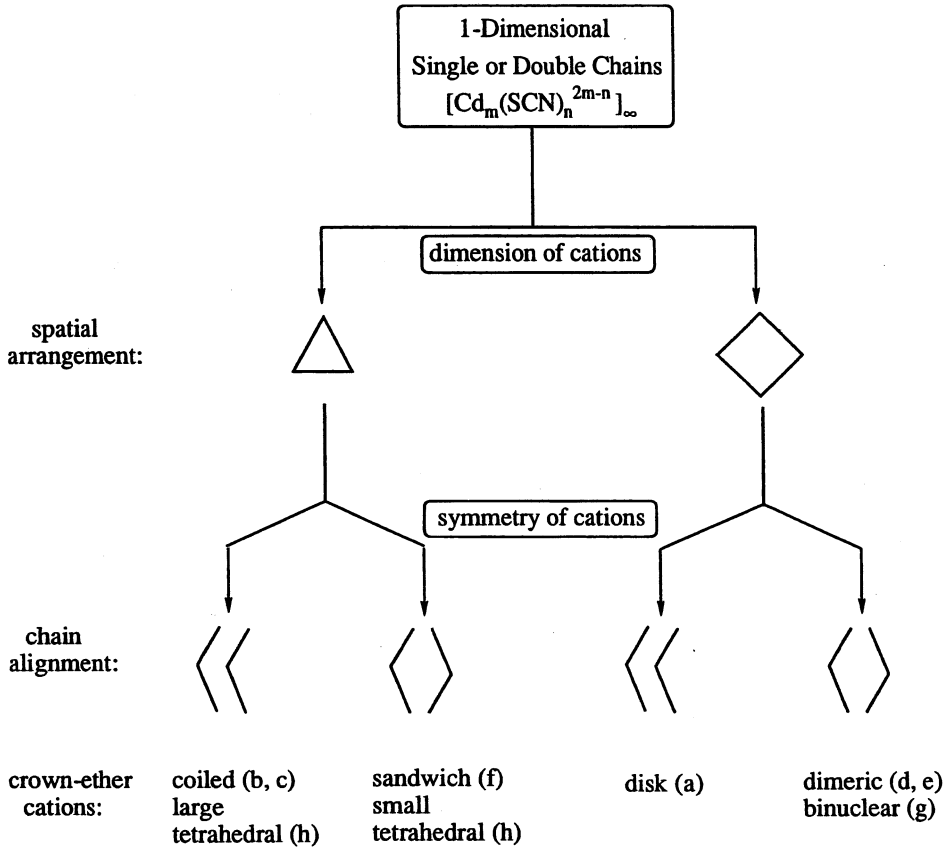

Chart 10.

triangular channels in **3** correspond to a single dimeric $[(18C6)_2Na_2(H_2O)_2]^{2+}$ dication in a square channel in **2** [1], both are per two $[Cd(SCN)_3^-]$ units.

However, size (volume) alone cannot explain why with $[(18C6)K]^+$ the anionic $[Cd(SCN)_3^-]_\infty$ chains in **1** also adopt the tetragonal arrangement. In fact, $[(18C6)K]^+$ (which has a volume of 300 Å^3) is somewhat smaller than $[(12C4)_2Na]^+$ (which is estimated to have a volume of 345 Å^3). The difference between these two cations is the geometrical shape. Since the channels formed by the anionic $[Cd(SCN)_3^-]_\infty$ chains must have dimensions large enough to accommodate the cations, the disk-like $[(18C6)K]^+$ cations, with a thickness of 4.0 Å and a diameter of 9.77 Å, require a tetragonal motif with an edge length of 10.62 Å and a diagonal dimension of $(2)^{1/2} \times 10.62$ Å $= 15.02$ Å. In fact, two $[(18C6)K]^+$ cations reside in each tetragonal channel (but at different heights with respect to the chain direction) with the lateral (diameter) dimension aligned with (i.e. parallel to) the diagonal of the square channel. This effect, exerted by the cations on the spatial arrangement of the anionic $[Cd(SCN)_3^-]_\infty$ chains, may be termed the 'dimension or geometrical effect'. This particular stereochemical characteristic persists in all the IPOS structures observed

so far and can also be extended to cations of different sizes and shapes as summarized in Table 1 and diagramatically in Chart 10. For example, with relatively small, tetrahedral cations such as $(Me_4N)^+$ and $(Et_4N)^+$, the $[Cd(SCN)_3^-]_\infty$ chains are also arranged in an approximate hexagonal array with the cations occupying the triangular channels in both $[Me_4N][Cd(SCN)_3]$ (**4**) and $[Et_4N][Cd(SCN)_3]$ (**5**) [10,11].

8.2. Cations as controllers (symmetry effect)

While dimensions (size and shape) of the cations can account for the spatial arrangement of the anionic infinite $[Cd(SCN)_3^-]_\infty$ chains (serving as spacers), the relative alignment (either parallel or antiparallel) is influenced by the symmetry or approximate symmetry of the cations, as depicted schematically in Chart 10. In this context, the cation serves as a controller of the crystal packing and crystal symmetry and may be termed the 'symmetry effect'. For NLO effects [5–7] such as SHG, it is important to arrange the chains in a parallel fashion in order to attain a noncentrosymmetric crystal symmetry. In other words, from a crystal engineering point of view, one should choose cations which are less prone to reside on inversion centers (-1 symmetry) or are in itself highly symmetrical or spherical in shape. In order to enhance the tendency of forming an acentric space group, the monomeric host–guest (1:1) complexes of either a disk-like, a partially coiled, or a coiled structure, as portrayed in Fig. 1(a–c), respectively, should be used as cationic spacer/controller. To prevent the formation of centric space groups, symmetrical cationic host–guest molecules such as dimeric structures (Fig. 1d,e), sandwich complexes (Fig. 1f), or two-nuclei complexes (Fig. 1g) should be avoided as these latter complexes have the tendency to form centrosymmetric structures. For example, cations such as the dimeric structures (e.g. $[(18C6)_2Na_2(H_2O)_2]^{2+}$ in **2**) can cause an antiparallel arrangement of the $[Cd(SCN)_3^-]_\infty$ chains whereas cations such as the disk-like complexes (e.g. $[(18C6)K]^+$ in **1**) can lead to a parallel arrangement of the $[Cd(SCN)_3^-]_\infty$ chains, resulting in centric and acentric space groups, respectively. In **3**, the sandwich $[(12C4)_2Na]^+$ monocation also favors an antiparallel arrangement of the $[Cd(SCN)_3^-]_\infty$ chains (though the cation itself conforms to D_{4d} symmetry which lacks the inversion symmetry), resulting in a centrosymmetric space group ($P2_1/n$).

The principle of symmetry control by the cations also applies to $[Me_4N][Cd(SCN)_3]$ (**4**) [10] and $[Et_4N][Cd(SCN)_3]$ (**5**) [11] mentioned previously. Here the tetrahedral $(Me_4N)^+$ and $(Et_4N)^+$ cations, which lack the inversion symmetry, give rise to noncentrosymmetric space groups $Pna2_1$ and $Cmc2_1$ for **4** and **5**, respectively. However, a detailed examination of these two latter structures indicate that the $[Cd(SCN)_3^-]_\infty$ chains in **4** and **5** are arranged in antiparallel and parallel fashions, respectively. We predict that the former should give rise to no (or weak) SHG effect while the latter should exhibit significant SHG effect. Hence, we conclude that noncentrosymmetry is a necessary but not sufficient condition for second-order NLO properties. Noncentrosymmetry must be augmented by parallel

alignment of the chains. In space groups such as $Cmc2_1$, the parallel alignment is guaranteed by the crystal symmetry of C-centering.

8.3. Cations as templates

An examination of the crystal structures of **8** and **9** prompted us to propose a 'templating mechanism' [2a] in which the organic host–guest cations serve as templates for the formation of the extended coordination solid structure, in a way similar to the formation of zeolite structures by organic template molecules [33]. In other words, we believe that the square-shaped $[(12C4)_2Cd]^{2+}$ dication 'induces' and/or 'directs' the formation of the intricate quilt composed of various basic building units (vide supra) woven into the observed tetragonal motif of the anionic $[Cd_2(SCN)_6^{2-}]_\infty$ polymeric structure (Fig. 10) for **8** and the hexagonal array of linear trimeric Cd_3 units arranged in a herringbone pattern with the $[Cd_3(SCN)_8^{2-}]$ complex as the building block (Fig. 14) for **9**.

A detailed comparison of the structures of **8** and **9**, however, reveals that while the $[(12C4)_2Cd]^{2+}$ dications in **8** are oriented in the upright position the $[(12C4)_2Cd]^{2+}$ dications in **9** are lying almost sideways with respect to the $[Cd_3(SCN)_8^{2-}]_\infty$ layers (see Fig. 18). This difference in the orientation of the $[(12C4)_2Cd]^{2+}$ dication with respect to the anionic cadmium-thiocyanate layers gives rise to the two distinct 2-D structures observed for **8** and **9**. This effect may be called 'anisotropic templating'. It is apparent that the observed anisotropy in the templating effect stems from the ability of the $[(12C4)_2Cd]^{2+}$ dications to align themselves either in the upright or the sideways orientations with respect to the anionic cadmium-thiocyanate layers.

9. From molecular host–guest complexes to crystal host–guest clathrates

In the 1-D cadmium-thiocyanate system, the infinite $[Cd(SCN)_3^-]_\infty$ zigzag chains create certain pattern of channels which are filled by the host–guest cationic molecules. Thus, the square channels created by the tetragonal arrangement of the $[Cd(SCN)_3^-]_\infty$ chains in $[(18C6)M][Cd(SCN)_3]$ ($M^+ = K^+$ (**1**), Na^+ (**2**)) [1a] are filled by the $[(18C6)K]^+$ (in **1**) or $[(18C6)_2Na_2(H_2O)_2]^{2+}$ (in **2**) cations, respectively. Similarly, the triangular channels created by the hexagonal array of $[Cd(SCN)_3^-]_\infty$ chains in **3** [1b] are filled with the sandwich $[(12C4)_2Na]^+$ cations. In this context, there is a close parallel between the 'molecular host–guest complexes' and 'crystal host–guest lattices'. For examples, the cations in **1** and **2** may be regarded as molecular host–guest complexes where the 'guest' alkali-metal ions (K^+ or Na^+) fit in the cavities of the crown-ether 'host', whereas the crystal structures may be considered as 'crystal host–guest clathrates' wherein the infinite $[Cd(SCN)_3^-]_\infty$ chains form an approximate square network of 'host lattice', creating square channels which are filled by molecular host–guest complex cations. The embedding of 'molecular host–guest complexes' as 'guest' in a host lattice to form a 'crystal host–guest clathrate' is rather interesting and may be considered as 'host–guest'

molecules within 'host–guest' lattices. The same concept applies to 1-D double-chain anionic cadmium-thiocyanate systems $[(15C5)_2Na_2(H_2O)_2]_{1/2}[Cd_2(SCN)_5]$ (**6**) and $[(15C5)K][Cd_2(SCN)_5]$ (**7**) [1c]. For 2-D anionic cadmium-thiocyanate coordination solids, a different kind of molecular host–guest complexes within crystal host–guest lattices is observed in which the cations are encapsulated (or 'intercalated') between the anionic cadmium-thiocyanate layers.

10. Advantageous properties of cadmium-thiocyanate systems as nonlinear optical crystals

The distinguishing features of the IPOS system, exemplified by the cadmium-thiocyanate coordination solids, as tailorable crystalline materials are:

1. the anions form isolated (well-separated) polymeric 1-D single chains such as $[Cd(SCN)_3^-]_\infty$, 1-D double chains such as $[Cd_2(SCN)_5^-]_\infty$, or 2-D networks such as $[Cd_2(SCN)_6^{2-}]_\infty$ and $[Cd_3(SCN)_8^{2-}]_\infty$,
2. the cationic host–guest complex serve as a spacer/controller of the crystal structure and crystal symmetry,
3. the extended π-conjugation system within the polymeric cadmium-thiocyanates, with the high polarizabilities of both the metal and the ligand, gives rise to desirable physical properties such as NLO effects,
4. the low dimensionality (e.g. 1- or 2-D) implies anisotropic physical properties,
5. low-lying π* orbitals of the SCN ligand give rise to strong metal-to-ligand charge-transfer (MLCT) excitation (or metal-mediated ligand $\pi \rightarrow \pi^*$ transitions),
6. Cd(II) d^{10} configuration gives rise to colorless crystals (transparent in the near ultraviolet regime (down to 220 nm), the entire visible spectrum, and the near infrared (up to 3.3 μm) region,
7. ionic $[H–G]^+[M–L]^-$ salts give rise to relatively high melting points and excellent chemical stabilities, good mechanical properties, and high radiation thresholds,
8. stoichiometric compounds of well defined structures,
9. flexibility in design and fabrication, and
10. amendable to large-dimension crystal growth, and ease of processing such as cutting and polishing.

Finally, though not emphasized in this review, one further potential of these coordination solids is that they can be cast into oriented thin films with highly anisotropic physical properties.

11. Concluding remarks and future prospects

General design strategies, in terms of symmetry control, as well as molecular and crystal engineering, in terms of electronic and stereochemical controls for NLO responses, have been formulated for the class of IPOS compounds involving 1- and

2-D cadmium-thiocyanate polymers. In particular, the crystal engineering principles developed here allows us to predict the spatial arrangement of the anionic cadmium-thiocyanate chains (geometry effect) and the relative alignment of the zigzag chains (symmetry effect) for 1-D single-chain $[Cd(SCN)_3^-]_\infty$ and double-chain $[Cd_2(SCN)_5^-]_\infty$ polymers, as well as to rationalize the different 2-D layered structures of $[Cd_2(SCN)_6^{2-}]_\infty$ and $[Cd_3(SCN)_8^{2-}]_\infty$, in terms of templating effect. It is hoped that these structural principles will allow the development of new strategies for materials fabrication at both molecular and crystal engineering levels as well as lead to the discoveries of other technologically useful materials.

Acknowledgements

The authors would like to thank the National Science Foundation (USA) for financial support of this research. They would also like to thank H. Zhu, W. Xiao, and H. Zang for their participation in this research.

References

[1] (a) H. Zhang, X. Wang, B.K. Teo, J. Am. Chem. Soc. 118 (1996) 11813. (b) H. Zhang, X. Wang, K. Zhang, B.K. Teo, Inorg. Chem. 37 (1998) 3490. (c) H. Zhang, X. Wang, K. Zhang, B.K. Teo, submitted for publication. (d) H. Zhang, X. Wang, K. Zhang, B.K. Teo, submitted for publication. (e) H. Zhang, D.E. Zelmon, G.E. Price, B.K. Teo, submitted for publication. (f) H. Zhang, X. Wang, B.K. Teo, submitted for publication.

[2] (a) H. Zhang, X. Wang, H. Zhu, W. Xiao, B.K. Teo, J. Am. Chem. Soc. 119 (1997) 5463. (b) H. Zhang, X. Wang, H. Zhu, W. Xiao, K. Zhang, B.K. Teo, submitted for publication.

[3] (a) C.J. Pedersen, J. Am. Chem. Soc. 89 (1967) 2495, 7017. (b) C.J. Pedersen, J. Org. Chem. 36 (1971) 254. (c) D.St.C. Black, I.A. McLean, Tetrahedron Lett. (1969) 3961. (d) J.M. Lehn, Acc. Chem. Res. 11 (1978) 49. (e) J.M. Lehn, Pure Appl. Chem. 49 (1977) 857. (f) J.M. Lehn, Struct. Bond. 16 (1973) 1. (g) D.J. Cram, J.M. Cram, Science 183 (1974) 803. (h) K. Madan, D.J. Cram, J. Chem. Soc. Chem. Commun. (1975) 427. (i) D.J. Cram, J.M. Cram, Acc. Chem. Res. 11 (1978) 8. (j) F. Vogtle (Ed.), Host–Guest Complex Chemistry I, II: Topics in Current Chemistry, vols. 98, 101, Springer-Verlag, Berlin, 1981, 1982.

[4] (a) M. Dobler, J.D. Dunitz, P. Seiler, Acta Crystallogr. B30 (1974) 2741. (b) M.A. Bush, M.R. Truter, J. Chem. Soc. Perkin Trans. 2 (1972) 345. (c) M. Dobler, R.P. Phizackerley, Acta Crystallogr. B30 (1974) 2748. (d) D.L. Hughes, J. Chem. Soc. Dalton Trans. (1975) 2374.

[5] (a) D.J. Williams (Ed.), Nonlinear Optical Properties of Organic and Polymeric Materials, ACS Symp. Ser. 233, American Chemical Society, Washington, DC, 1983. (b) D.J. Williams, Angew. Chem. Int. Ed. Engl. 23 (1984) 690. (c) S.R. Marder, J.E. Sohn, G.D. Stucky (Eds.), Materials for Nonlinear Optics: Chemical Perspectives, ACS Symp. Ser., 1991, p. 455. (d) S.D. Cox, T.E. Gier, G.D. Stucky, J. Bierlein, J. Am. Chem. Soc. 110 (1988) 2986. (e) Y.R. Shen, The Principles of Nonlinear Optics, Wiley, New York, 1984. (f) F. Zernike, J.E. Midwinter, Applied Nonlinear Optics, Wiley, New York, 1973.

[6] (a) D.R. Kanis, M.A. Ratner, T.J. Marks, J. Am. Chem. Soc. 114 (1992) 10338. (b) T.J. Marks, G.K. Wong, D. Dai, M.A. Hubbard, N. Minami, J.W. Park, J. Yang, Abs. Pap. ACS 199 (1990) 194. (c) D. Li, M.A. Ratner, T.J. Marks, J. Am. Chem. Soc. 110 (1988) 1707. (d) B.F. Levine, C.G. Bethea, Appl. Phys. Lett. 24 (1974) 445. (e) G.R. Meredith, Opt. Commun. 39 (1981) 89. (f) F. Kajzar, J. Messier, Phys. Rev. A 32 (1985) 2352. (g) L.-T. Cheng, W. Tam, S.H. Stevenson, G.R. Meredith, J. Chem. Phys. 95 (1991) 10631.

[7] (a) S.R. Marder, L.T. Cheng, B.G. Tiemann, J. Chem. Soc. Chem. Commun. (1992) 672. (b) J.C. Calabrese, L.T. Cheng, J.C. Green, S.R. Marder, W. Tam, J. Am. Chem. Soc. 113 (1991) 7227. (c) S. Gilmour, S.R. Marder, B.G. Tiemann, L.-T. Cheng, J. Chem. Soc. Chem. Commun. (1993) 432. (d) K.S. Suslick, C.T. Chen, G.R. Meredith, L.-T. Cheng, J. Am. Chem. Soc. 114 (1992) 6928. (e) F. Meyers, J.L. Bredas, J. Zyss, J. Am. Chem. Soc. 114 (1992) 2914. (f) B.G. Tiemann, S.R. Marder, J.W. Perry, L.T. Cheng, Chem. Mater. 2 (1990) 690. (g) J. Zyss, J. Chem. Phys. 70 (1979) 3333. (h) J. Zyss, J. Mol. Electron. 1 (1985) 25. (i) M. Barzoukas, M. Blanchard-Desce, D. Josse, J.-M. Lehn, J. Zyss, J. Chem. Phys. 133 (1989) 323. (j) K. Kajikawa, T. Anzai, H. Takezoe, A. Fukuda, S. Okada, H. Matsuda, H. Nakanishi, T. Abe, H. Ito, Appl. Phys. Lett. 62 (1993) 2161. (k) K. Kajikawa, T. Anzai, H. Takezoe, A. Fukuda, S. Okada, H. Matsuda, H. Nakanishi, T. Abe, H. Ito, Chem. Phys. Lett. 192 (1992) 113.
[8] A.A. Newman (Ed.), Chemistry and Biochemistry of Thiocyanic Acid and its Derivatives, Academic Press, New York, 1975.
[9] A.M. Golub, H. Kohler, V.V. Skopenko (Eds.), Chemistry of Pseudohalides, Elsevier, Amsterdam, 1986.
[10] Y. Kuniyasu, Y. Suzuki, M. Taniguchi, A. Ouchi, Bull. Chem. Soc. Jpn. 60 (1987) 179.
[11] M. Taniguchi, A. Ouchi, Bull. Chem. Soc. Jpn. 62 (1989) 424.
[12] M. Taniguchi, A. Ouchi, Bull. Chem. Soc. Jpn. 60 (1987) 4172.
[13] V.G. Thiele, D. Messer, Z. Anorg. Allg. Chem. 464 (1980) 255.
[14] R. Gronbaek, J.D. Dunitz, Helv. Chim. Acta 47 (1964) 1889.
[15] G.R. Desiraju, Crystal Engineering, Elsevier, New York, 1989, Ch. 8.
[16] G.D. Stucky, J.E. Mac Dougall, Science 247 (1990) 669.
[17] F. Meyer, J.L. Bredas, J. Zyss, J. Am. Chem. Soc. 114 (1992) 2914.
[18] Y. Aoyama, K. Endo, T. Anzai, Y. Yamaguchi, T. Sawaki, K. Kobayashi, N. Kanehisa, H. Hashimoto, Y. Kai, H. Masuda, J. Am. Chem. Soc. 118 (1996) 5562.
[19] R.E. Melendez, C.V.K. Sharma, M.J. Zaworotko, C. Bauer, R.D. Rogers, Angew. Chem. Int. Ed. Engl. 35 (1996) 2213.
[20] B.F. Hoskins, R. Robson, J. Am. Chem. Soc. 112 (1990) 1546.
[21] C.B. Aakeroy, D.P. Hughes, M. Nieuwenhuyzen, J. Am. Chem. Soc. 118 (1996) 10134.
[22] G.C. Kulasingam, W.R. McWhinnie, J. Chem. Soc. A (1968) 254.
[23] (a) R.G. Pearson, J. Am. Chem. Soc. 85 (1963) 3533. (b) R.G. Pearson, Adv. Inorg. Chem. Radiochem. 8 (1966) 177. (c) F. Basolo, Coord. Chem. Rev. 3 (1968) 213. (d) J.L. Burmeister, Chem. Rev. 3 (1968) 225.
[24] J.L. Burmeister, in: A.A. Newman (Ed.), Chemistry and Biochemistry of Thiocyanic Acid and Its Derivatives, Academic Press, New York, 1975, Ch. 2.
[25] (a) P.C. Jain, E.C. Lingafelter, P. Paoletti, J. Am. Chem. Soc. 90 (1968) 519. (b) G.D. Andreetti, P.C. Jain, E.C. Lingafelter, J. Am. Chem. Soc. 91 (1969) 4112.
[26] M. Cannas, G. Carta, A. Cvistini, G. Marongiu, J. Chem. Soc. Dalton Trans. (1976) 210.
[27] C. Gagnon, A.L. Beauchamp, Acta Crystallogr. B35 (1979) 166.
[28] (a) D.V. Naik, W.R. Scheidt, Inorg. Chem. 12 (1973) 272. (b) P.I. Lazarev, L.A. Aslanov, M.A. Porai-Kosic, V.M. Ionov, Koord. Chim. B (1975) 710. (c) G. Bombieri, P.T. Moselev, D. Brown, J. Chem. Soc. Dalton Trans. (1975) 1520. (d) P.I. Lazarev, L.A. Aslanov, M.A. Porai-Kosic, Koord. Chim. 1 (1975) 479.
[29] D.W. Meek, P.E. Nicpon, V.I. Meek, J. Am. Chem. Soc. 92 (1970) 5351.
[30] G.J. Palenik, W.L. Steffen, M. Mathew, M. Li, D.W. Meek, Inorg. Nucl. Chem. Lett. 10 (1974) 125.
[31] U.A. Gregory, J.A. Jarvis, B.T. Kilbourn, P.G. Owston, J. Chem. Soc. A (1970) 2770.
[32] J.M. Homan, J.M. Kawamoto, G.L. Morgan, Inorg. Chem. 9 (1970) 2533.
[33] The use of (crown-ether)–(alkali-metal) complexes as templates in the synthesis of zeolite crystals is well established. See, for example, F. Delprato, L. Delmotte, J.L. Guth, L. Huve, Zeolites 10 (1990) 546.
[34] (a) L.A. Aslanov, V.M. Ionov, S.S. Sotman, Kristallografija 21 (1976) 1198. (b) M. Cannas, G. Carta, A. Cvistini, G. Marongiu, J. Chem. Soc. Dalton Trans. (1976) 300. (c) A.L. Beauchamp, D. Goutier, Can. J. Chem. 50 (1972) 977.

[35] J.W. Jeffrey, K.M. Rose, Acta Crystallogr. B24 (1968) 653.
[36] A.M. Porai-Kosic, Z. Strukt. Chim. 4 (1963) 584.
[37] R. Makhija, L. Pazdernik, R. Rivest, Can. J. Chem. 51 (1973) 438.
[38] M. Iizuka, T. Sudo, Z. Kristallogr. 126 (1968) 376.
[39] (a) W. Sturmer, U. Deserno, Phys. Lett. A32 (1970) 539. (b) D. Yuan, D. Xu, M. Liu, F. Qi, W. Yu, W. Hou, Y. Bing, S. Sun, M. Jiang, Appl. Phys. Lett. 70 (1997) 544.
[40] The majority of organic NLO materials with large hyperpolarizabilities consist of a conjugated system containing a donor and an acceptor groups positioned at both ends of the conjugation—see Refs. [5–7]. However, the presence of polarizing groups of this type usually causes the molecules to crystallize in a centrosymmetric space group and the NLO effect is reduced or lost (see, however, work by Whitesell and coworkers refuting this notion. Furthermore, in one particular SHG application from 830 nm (a semiconductor diode laser) to the second harmonic of 415 nm, polar molecules of this type show a strong absorption either near UV or in the visible region of the spectrum, producing destructive absorption of the required wavelength [41]).
[41] J.K. Whitesell, R.E. Davis, L.L. Saunders, J. Am. Chem. Soc. 112 (1991) 3267.
[42] Z. Kotler, R. Hierle, D. Josse, J. Zyss, R. Masse, J. Opt. Soc. Am. B 9 (1992) 534.
[43] S.K. Kurtz, T.T. Perry, J. Appl. Phys. 39 (1968) 3798.